6-1-2013

Rechargeable battery modeling and lifetime optimization

Naglaa El Agroudy

The American University in Cairo

School of Sciences and Engineering

RECHARGEABLE BATTERY MODELING AND LIFETIME OPTIMIZATION

A Thesis Submitted to

Electronics Engineering Department

in partial fulfillment of the requirements for
the degree of Master of Science

by Naglaa El Agroudy

under the supervision of Prof. Yehea Ismail
May/2013

ACKNOWLEDGEMENTS

First and foremost, I thank ALLAH the Almighty for providing me with strength, persistence and patience to complete this work.

I wish to express my high appreciation and sincere gratitude to Dr. Yehea Ismail for his valuable supervision, guidance and continuous encouragement during supervision of this work.

Finally, I would like to thank my family, my parents, my husband, my work colleagues and classmates who always supported me and kept encouraging me to do better.

ABSTRACT

The American University in Cairo

Rechargeable Battery Modeling and Lifetime Optimization

Naglaa El Agroudy

Thesis Advisor: Dr. Yehea Ismail

Battery lifetime is one of the most important design considerations in rechargeable battery operated devices. Understanding the battery nonlinear properties is essential for appropriate battery modeling. Optimizing the battery lifetime depends greatly on the discharge current profile. Changing the profile shape can be done through averaging techniques, scheduling techniques, introducing recovery periods…etc. This work investigates the different techniques that can be used to enhance the battery lifetime. It is shown that 15-60% of lifetime savings can be achieved through using average current profile instead of variable current profile. This work also provides a comparison between different configuration techniques for multi-cell systems. Also, a new hybrid battery model is introduced which combines the battery electric circuit characteristics together with the nonlinear battery properties.

TABLE OF CONTENTS

LIST OF FIGURES

LIST OF TABLES

I. INTRODUCTION

A. Motivation of Work

Many electronic devices and equipment are now depending on rechargeable batteries for their operation. Rechargeable batteries are able to store energy then deliver it to the attached load whenever needed. The main concern for the designers of battery operated systems is how to increase the lifetime of the battery. This can be done through many techniques like increasing the number of cells, optimizing the battery discharge profile, introducing idle periods for the battery to recover…etc. The battery has a nonlinear operation which means that the relation between the load current and the lifetime of the battery is not linear. The capacity that can be extracted from the battery depends greatly on the discharge load current profile [1]. In order to optimize the battery lifetime, many battery properties need to be understood. This work presents a study about the different battery nonlinear properties and the different models that are used to represent these properties. This work presents a study for single and multi cell battery systems and a study for different configurations of connecting the battery cells and decides which of them is better for the system lifetime. Also, this work introduces a new hybrid battery model that takes into consideration the battery nonlinear behavior together with the battery electric characteristics.

The remainder of this chapter will include literature review about the different battery properties, battery models and battery life time optimization techniques. The next chapters will be organized as follows: in chapter two, Lithium ion battery study for single cell will be conducted. In chapter three, a new hybrid battery model is introduced that includes the characteristics of both the electric circuit models and the analytical diffusion nonlinear model. Chapter four will include simulation results and observations for single cell lithium ion battery. Chapter five will include the multi-cell system study and the comparison between different cell operating configurations and studying which configuration is better for increasing the lifetime.

B. LITERATURE REVIEW

1. Battery Properties

Rechargeable batteries have many properties that define their charging/discharging characteristics. Ideally, for any discharge current, the battery capacity should stay constant [1]. All the energy stored in the battery should be totally consumed till the battery is empty. During discharge, the battery voltage is expected to be constant and it should drop to zero when the battery is fully discharged [1]. However, in reality, batteries behavior is highly nonlinear. To understand this nonlinear behavior, the following battery properties are going to be discussed in detail.

a. Battery capacity

The amount of electric charge that can be stored inside a battery is known as the capacity. It is measured in Ampere-Hour unit, which means that if the battery capacity is 3 A.H, then if the battery is discharged with a constant 3A current, then it will be completely discharged after one hour. Batteries are characterized by two voltages. When the battery is fully charged, its initial voltage is called the open circuit voltage (V_{oc}), and when it is fully discharged, its final voltage is called cut off voltage (V_{cutoff}) [2]. There are three ways to describe the battery capacity. The first definition is the theoretical capacity which represents the total amount of energy that can be extracted from the battery. The second definition is the standard capacity, which represents the amount of energy that can be extracted from the battery if standard loads are used to discharge it. The battery manufacturer specifies those standard loads. The third definition is the actual capacity of the battery, which is the amount of energy that can be extracted when a given load is used to discharge it. The battery efficiency is determined by the actual capacity of the battery and its lifetime. A system is battery efficient when it can get an improved actual capacity utilizing certain discharge profile characteristics of the actual application [2]. Understanding the battery capacity allows us to define the State of Charge (SOC) which is the percentage of the available capacity of the battery with respect to the maximum

available battery capacity. So the SOC is 100% if the battery is fully charged, and it is 0% when it is fully discharged.

b. Rate capacity effect

The energy stored in a battery is the product of its voltage (V) by its capacity (Ampere-Hour). As mentioned earlier, in an ideal battery, the voltage remains the same during the whole discharge time and then drops to zero when the battery is completely empty. Also, for all load currents, the battery capacity is ideally constant. However, in reality, this behavior is different. During discharge, the battery voltage drops in a nonlinear fashion. The higher the battery load, the lower the battery effective capacity. This phenomenon is known as the rate capacity effect [1]. This is due to the non-uniformity of the inactive reaction site distribution at the battery electrodes [2]. When the rate of discharge is low, the inactive reaction sites distribution is uniform. However, when a large current is drawn (i.e. rate of discharge is high), reduction occurs only at the outer surface of the cathode. An insoluble compound is formed on the cathode surface which hinders the active internal reaction sites. Despite the unutilized active cathode sites, the battery will appear as discharged [2].

c. Recovery effect

Battery can recover part of its lost capacity if it is left idle or is discharged very slowly. This results in an increase in the effective capacity and consequently the lifetime. At idle periods, the positive lithium Li^+ ions concentration is uniform at the interface of the electrode with the electrolyte [2]. Li^+ ions are consumed at the cathode-electrolyte interface (reduction reaction) during discharging and they are replaced with new Li^+ ions that are released from the anode (oxidation reaction) into the electrolyte. When the rate of discharge is high (i.e. large current drawn), the rate at which the positive ions are consumed at the cathode becomes much higher than the rate with which the ions are released at the anode [2]. This will result in a non-uniform concentration gradient of the lithium ions in the electrolyte [3]. When the battery is allowed some idle time to recover, the lithium ions will diffuse through the electrolyte till their gradient becomes zero again.

Li^+ ions will be uniformly distributed again; however their concentration will be less than that of a fully charged battery. When the concentration of the ions drops below a certain level, the battery will be declared as discharged as the electrodes reaction will no longer be able to take place [3].

d. Aging

As the battery charge/discharge cycles increase, the actual capacity of the battery decreases, which is known as the aging effect [4]. This relationship is shown in Figure 1. This results in a lower lifetime for the battery for a given load. It was shown that during the first 450 charge/discharge cycles, 10-40% decrease happens in the deliverable capacities of the battery. One of the main causes of aging is cell oxidation which leads to film growth on the electrode [4]. This increases the battery internal resistance. This effect is nonreversible and it finally leads to battery failure.

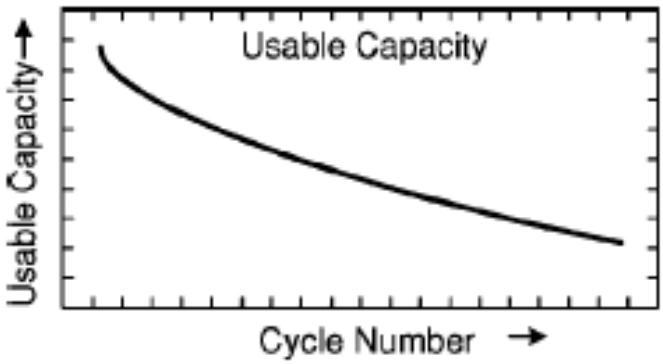

Figure 1: Usable Capacity vs. Cycle Number [5]

Besides cell oxidation, complex battery operating conditions can expedite the aging process as well [6]. The aging process is affected by the temperature condition: the higher the temperature, the faster the aging process. For example, battery can operate for 2000 cycles at room temperature (25°*C)* but it can only operate for 800 cycles at 55°*C* [5].

Also, as the depth of discharge increases and as the current cycle profile becomes demanding, the aging process speeds up [6]. The aging effect indicator is called the state of health of the battery (SOH) which can be determined by measuring the battery

impedance or conductance [7]. SOH is an indicator of how much capacity the battery is able to deliver compared to a new battery. It is defined as [7]

$$SOH = \frac{Q_{max\_aged}}{Q_{\max\_new}} \qquad \text{Equation 1}$$

Where Q_{max_aged} is the maximum charge capacity of an aged battery, and Q_{max_new} is the maximum charge capacity of a new battery. When the SOH goes below 80%, the battery is assumed to be in mild fault condition.

e. Temperature

Temperature highly affects the battery cycle life, where the cycle life is defined as the time the battery takes to go from a fully charged to a fully discharged state where its voltage reaches the cutoff voltage [4]. Electrolyte conductivity, electrolyte diffusion coefficients and the rate of electrochemical reactions are all properties of the battery material that are affected by temperature [5]. The battery internal chemical reactions slow down and its internal resistance increases when the battery operation happens in a temperature below the room temperature (below 23°C). This results in lower capacity delivered by the battery and higher voltage discharge curve [8]. However, if the temperature is higher than the room temperature, the internal chemical reactions rate increases which reduce the battery actual capacity if it is stored in the high temperature. It is found that it is best for the battery to operate in a temperature near the room temperature to improve aging [9].

f. Self-Discharge

Internal chemical reactions that take place inside the battery while being stored lead to loss in the battery stored charge. This phenomenon is known as the self-discharge. The type of the battery, the storage temperature and the state of charge all affect the self-discharge rate. Figure 2 shows how the battery usable capacity decreases as the storage time increases.

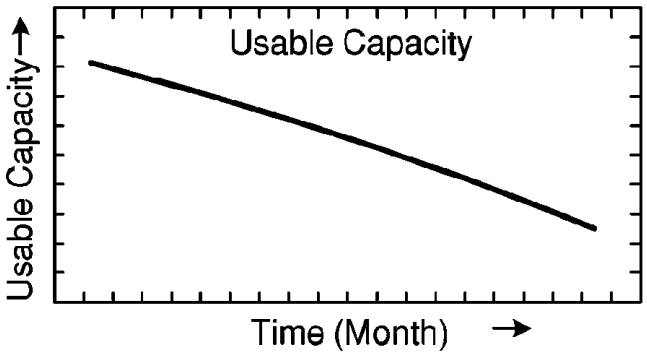

Figure 2: Usable Capacity vs. Storage Time [5]

2. Battery Models

This section discusses the different battery models that are surveyed in literature. There are electrochemical models, electric models, analytical models, mathematical models and stochastic models. Each of these models varies in complexity as it takes into account certain battery properties that serve a certain purpose. The models may be used for battery design, circuit simulation or performance estimation. We will discuss each of these models in detail.

a. Electrochemical Models

Electrochemical models are assumed to be the most complex models as they use six coupled time variant partial differential equations that are very difficult and time consuming to simulate [1,5]. Complex numerical algorithms are used to optimize the battery design aspects and relate both voltage and current information with the concentration distribution information [5]. The highly detailed description used by these models makes them the most accurate to describe battery processes as they are based on chemical processes that take place inside the battery, but in the same time it makes them very complex and difficult to use [1, 2, 10]. The most known electrochemical model for lithium ion cells is developed by Doyle et al [11]. This model is available in a Fortran program called Dualfoil that is used to simulate lithium ion batteries. Dual foil is available for free on the internet. For an input load profile from the user, Dualfoil can simulate all the changes in battery properties that

happen over time. However, very good detailed knowledge about the battery is needed by the user to be able to set fifty other battery parameters for Dualfoil like overall heat capacity, electrodes thickness, and initial salt concentration in the electrolyte…etc. Due to the high accuracy of the program, it is often used as a comparison against other models instead of using experimental results [1, 3, 8].

b. Electrical Circuit Models

Battery electrical properties are modeled by SPICE circuits using voltage sources, look up tables, resistors and capacitors. Most of the electrical circuit models are characterized by the following [1]:

- A capacitor to model the battery capacity.
- At high discharge currents, lost capacity is determined using a discharge rate normalizer.
- Load circuit to discharge the battery capacity.
- Look up table for the voltage vs. state of charge.
- Resistor to model the battery resistance.

The electrical circuit models require some effort to configure as battery experimental data is required to develop the look up table. Also, they are less accurate than electrochemical models. They can have errors up to 12% in predicting battery lifetime. However, they are much simpler than the electrochemical models and computationally less complex [1]. There are three basic categories of the electrical circuit models: Thevenin, impedance, and runtime-based models [5].

i. Thevenin-Based Electrical Model

Thevenin based model as shown in Figure 3, uses series resistor (R_{Series}) and an RC parallel network ($R_{Transient}$ and $C_{Transient}$) to predict the battery response at a particular state of charge to transient load events. It assumes a constant open circuit voltage V_{OC}(SOC). However, this assumption makes the model unable to give the battery voltage variations in steady state and its runtime information [5]. Some efforts were done to improve this disadvantage by adding additional components that take

into effect the runtime and the steady state response of the battery voltage. In [12] V_{OC}(SOC) is replaced by a variable capacitor representing the nonlinear V_{OC} and SOC. However, this complicates the computation of SOC as it needs to integrate over the voltage which is now variable based on the variable capacitor. This model gives 5% runtime error and 0.4V error in voltage value for constant charge and discharge currents. In [13], the nonlinear relationship between V_{OC} and SOC is modeled but the transient behavior is ignored. In [14-16] additional mathematical equations are needed to compute the SOC and estimate runtime, and they are not implemented in circuit simulators. [17] used the battery physical process to extract a complicated electrical network that represents the open-circuit voltage (V_{OC}) which complicates the whole model. All the above discussed Thevenin based models are unable to predict the battery lifetime in a simple accurate way in circuit simulators.

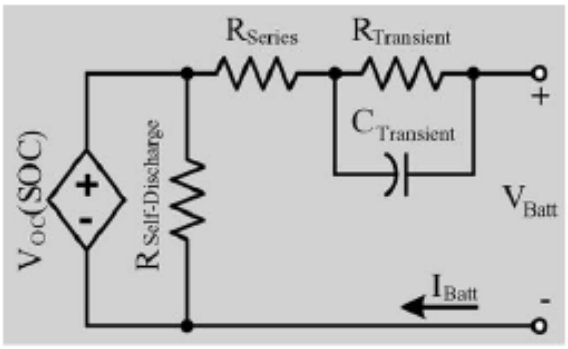

Figure 3: Thevenin Based Electrical Battery Model [5]

ii. Impedance-Based Electrical Model

Impedance based models, as shown in Figure 4, uses an ac equivalent impedance model Z_{ac} to model the AC battery behavior. This complicated Z_{ac} network has to fit the impedance spectra which is a very difficult and complex process [5]. Another disadvantage of this model is that it is not able to predict the dc response of the battery or the lifetime as it can only work for a fixed temperature setting and fixed SOC [5,18].

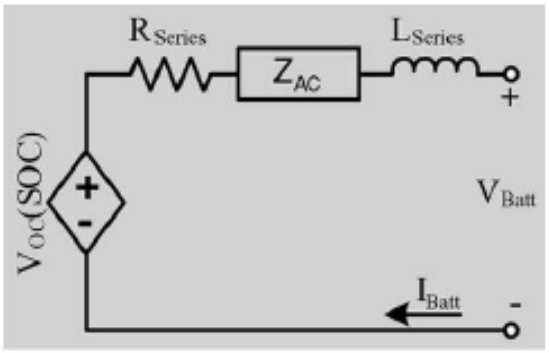

Figure 4: Impedance Based Electrical Battery Model [5]

iii. Runtime-Based Electrical Model

Using a complex circuit network, the runtime based electrical models (Figure 5) can simulate the battery lifetime and the dc response for constant loads in SPICE compatible simulators [5]. However those models cannot estimate accurately the battery lifetime or the voltage response for varying loads. Table 1 shows comparison between the different electrical models. This comparison indicates that none of these models can be implemented in circuit simulators to predict both the battery lifetime and *I*–*V* performance accurately [5].

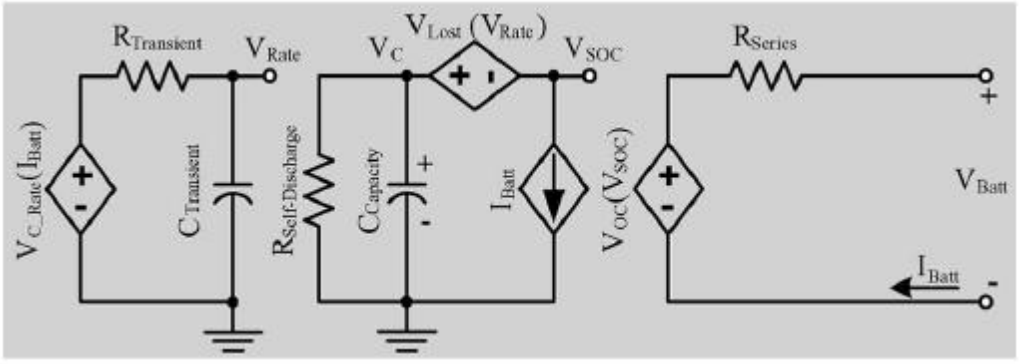

Figure 5: Runtime Based Electrical Battery Model [5]

Table 1: Comparison of Electrical Circuit Models [5]

Predicting Capability	Thevenin Based Model	Impedance Based Model	Runtime Based Model
DC	No	No	Yes
AC	Limited	Yes	No
Transient	Yes	Limited	Limited
Battery Runtime	No	No	Yes

iv. Comprehensive Electrical Battery Model

This model, developed by Min Chen et al., combines the transient capabilities of Thevenin based models, AC features of impedance-based models, and runtime information of runtime based model. The model is shown in Figure 6. The $C_{capacity}$ capacitor and the current controlled current source model the capacity, state of charge and the battery run time. Those components are inherited from the run time based models. The RC network that simulates the transient response is inherited from the Thevenin based models. A voltage controlled voltage source is used to relate the SOC to the open-circuit voltage. This model is a SPICE compatible model and can predict the battery runtime, steady state and transient response accurately. It captures the battery electrical characteristics: usable capacity ($C_{capacity}$), open circuit voltage (V_{OC}) and the transient response (RC network).

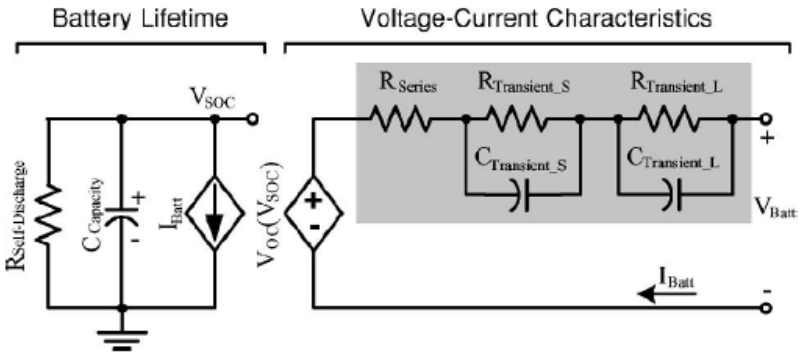

Figure 6: Comprehensive Electrical Battery Model [5]

The total charge stored in the battery (SOC) is represented by the capacitor $C_{Capacity}$ which is obtained by converting the nominal battery capacity in Ampere.Hour to charge in Coulomb.

$$C_{Capacity} = 3600 \cdot Capacity \cdot f1(Cycle) \cdot f2(Temp) \qquad \text{Equation 2}$$

Where Capacity is the nominal capacity in Ampere Hour and f1 (Cycle) and f2 (Temp) are cycle number- and temperature-dependent correction factors.

The battery can be initialized to be fully charged or fully discharged by setting the initial voltage across $C_{Capacity}(V_{SOC})$ to be equal to 1 V or 0 V. The SOC of the battery is thus represented quantitatively by the V_{SOC}. Figure 7 shows that the battery capacity varies with its current. Different currents owing to different voltage drops across the battery internal resistance lead to different state of charge values at the end of the discharge cycle which causes the variation of the capacity with the current [5].

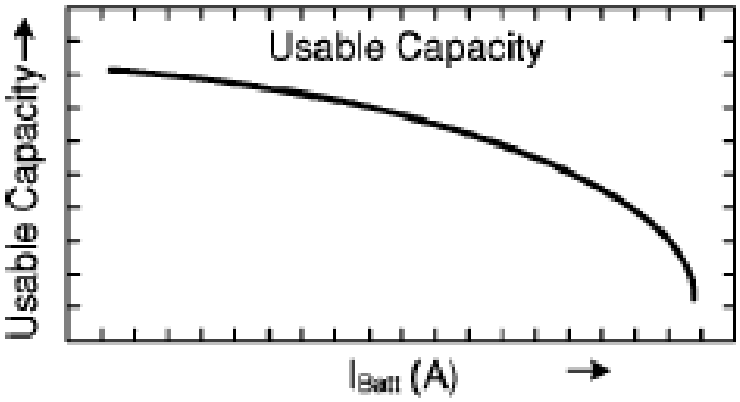

Figure 7: Usable Capacity vs. Battery Current [5]

During battery charging/discharging, the current-controlled current source I_{Batt} charges or discharges the capacitor $C_{Capacity}$ and as a result, the state of charge will change dynamically due to the change in V_{SOC}. Thus, the battery lifetime can be determined when the battery voltage reaches the end of discharge voltage. The self discharge that happens when batteries are stored for long time is represented with the self-discharge resistor $R_{Self\text{-}Discharge}$. $R_{Self\text{-}Discharge}$ is a function of SOC, temperature, and cycle number. The capacity retention curve shows that when no load is connected to the battery, the usable capacity decreases slowly with time (Figure 2) and thus the self discharge effect can be simplified as a large resistor or even ignored.

There is a non-linear relation between V_{OC} and SOC as shown in Figure 8. The voltage-controlled voltage source $V_{OC}(V_{SOC})$ is used to represent this relation.

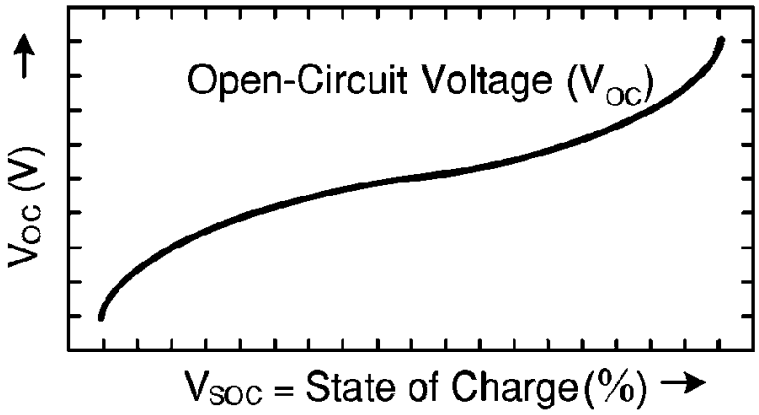

Figure 8: Non-linear relation between Voc and Vsoc [5]

The step response to a current event is shown in Figure 9 where the battery voltage responds slowly. The shaded RC network in Figure 6 represents the transient response of the battery. The instantaneous voltage drop of the step response is modeled by the series resistor R_{series}. The short and long time constants of the step response are accounted for by $R_{Transient\_S}$, $C_{Transient\_S}$, $R_{Transient\_L}$, and $C_{Transient\_L}$.

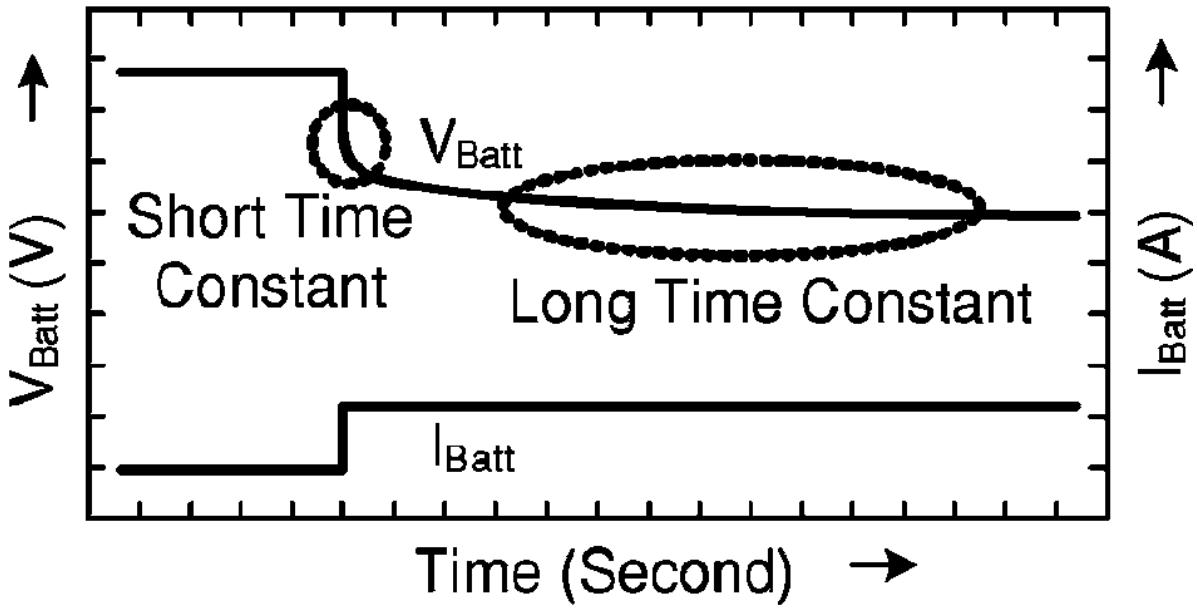

Figure 9: Transient Response to a Step Load-Current Event [5]

Based on numerous experiments, two RC time-constants are used instead of one or three or more. This is a tradeoff between accuracy and complexity and it keeps the error within 1mV for all the curve fittings.

c. Stochastic Models

The stochastic models use Markovian processes with probabilities to describe the battery behavior and the recovery effect. According to the physical characteristics of the battery, the probabilities are expressed in terms of parameters that are related to them [19-22]. A stochastic kinetic battery model was developed in [20-21]. In this model, since the lifetime of the battery highly depends on the load current frequency, therefore the recovery probability during idle periods is made dependent on the length of the idle periods. Another model describes the behavior of lithium ion batteries under pulsed discharge current is shown in Figure 10 [22]. This model uses a decreasing exponential function of the state of charge and discharge capacity to model the battery recovery effect. The discharge demand is assumed to be a Bernoulli driven stochastic process with Poisson distribution. The results of this model are compared to the results of the electrochemical model. The results show that the model has 4% maximum deviation from the electrochemical model with 1% average deviation. It also shows that a good qualitative description of the battery behavior is modeled under pulsed discharge current but no quantitative data is available as its results are in terms of only the gain and no number for the computed lifetime [1]. Also, the model does not handle the battery nonlinearity and variable discharge current profiles.

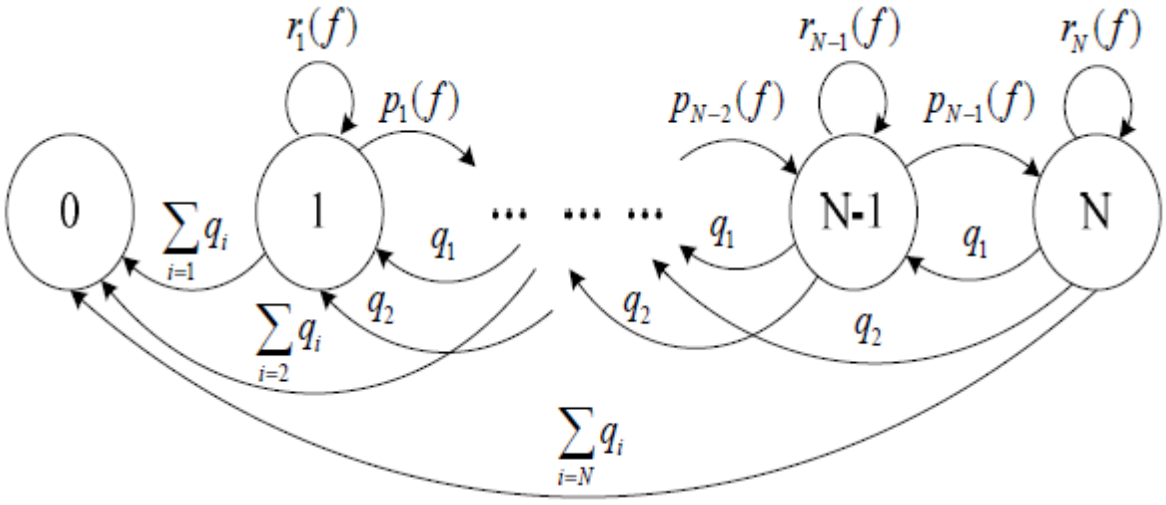

Figure 10: Stochastic Process Representing the Cell Behavior [22]

d. Analytical Models

i. Peukert's Law

This law is the simplest analytical battery model where the lifetime under a constant load is represented by [3]:

$$L = \frac{a}{I^b} \qquad \textbf{Equation 3}$$

Where L is the lifetime, I is the discharge current, a (battery capacity) and b (Peukert's constant) are appropriate coefficients. However, for variable discharge current, this law does not hold. With this law, all load profiles with the same average current will have the same battery lifetime, which is experimentally not true. So this law holds only for constant loads and fails with variable loads.

ii. Kinetic Battery Model

Manwell and McGowan developed the KiBaM [23-25] where it uses the chemical kinetics process as its basis and hence the name Kinetic. In Figure 11 below, the model uses two wells over which the battery charge is distributed. The first well is the available charge well and the second is the bound charge well.

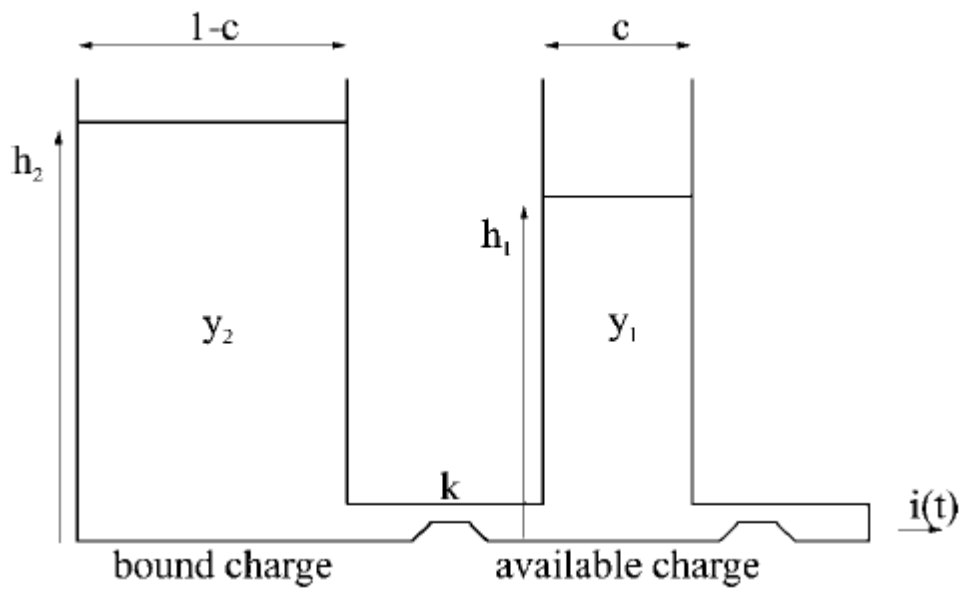

Figure 11: Kinetic Battery Model [1]

The available charge well denoted with $y_1(t)$ has a fraction c of the total capacity, where a fraction 1- c is in the bound charge well denoted with $y_2(t)$. The load i(t) is supplied directly with electrons from the available charge well and those electrons are then substituted with another ones from the bound charge well. In between the two wells, there is a valve with fixed conductance *k*. The height difference between the two wells determines the rate at which charge flows between them. The heights are given by [1]:

$$\boldsymbol{h_1 = \frac{y_1}{c}} \qquad \textbf{Equation 4}$$

$$\boldsymbol{h_2 = \frac{y_2}{1-c}} \qquad \textbf{Equation 5}$$

The following differential equations system describes the change of the charge in the two wells [1]:

$$\begin{cases} \boldsymbol{\frac{dy_1}{dt} = -i(t) + k(h_2 - h_1)} \\ \boldsymbol{\frac{dy_2}{dt} = -k\,(h_2 - h_1)} \end{cases} \qquad \textbf{Equation 6}$$

With initial conditions: $y_1(0) = c \cdot C$ and $y_2(0) = (1 - c).C$, where C is the total battery capacity. When the available charge well becomes empty, the battery is considered fully discharged. The height difference between the two wells increases when a load is applied to the battery as the available charge then decrease. When the load is removed, the two heights become equal again as the charge flows from the bound charge well to the available charge well. So the battery recovers some of its charge during idle times and will last longer than the case of applying continuous load with no idle periods. Besides the recovery effect, this model also takes into account the rate capacity effect. The available charge well will be drained faster with higher discharge current as the flow of charge from the bound well to the available well will not be able to cope with the fast charge drainage [1]. Therefore the battery effective capacity will be lower as more charge in the bound well will remain unused. The differential equations (6) can be solved for the case of a constant discharge current [i(t) = I] using Laplace transforms, which yields [1] :

$$\begin{cases} y_1(t) = y_{1,0}e^{-k't} + \frac{(y_0k'c-I)(1-e^{-k't})}{k'} - \frac{Ic(k't-1+e^{-k't})}{k'} \\ y_2(t) = y_{2,0}e^{-k't} + y_0(1-c)(1-e^{-k't}) - \frac{I(1-c)(k't-1+e^{-k't})}{k'} \end{cases}$$

Equation 7

Where k' is defined as $k' = \frac{k}{c(1-c)}$, $y_{1,0}$ and $y_{2,0}$ are the amount of available and bound charge, respectively, at t = 0, and $y0 = y_{1,0} + y_{2,0}$.

iii. Rakhmatov Diffusion Model

This model was developed by Rakhmatov and Vrudhula [3]. When the battery is discharged, the electrons are released from the anode to the external circuit (oxidation), while the cathode accepts electrons from the circuit (reduction) as shown in Figure 12.

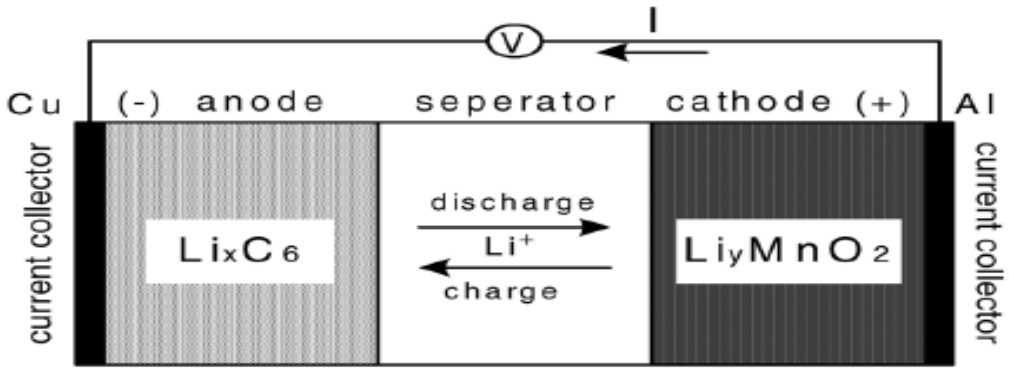

Figure 12: Lithium Ion Battery Operation [4]

The chemical processes are reversed when the battery is charged. The electrochemical phenomena that happens inside the battery is treated by this model at a high abstraction level which makes the model less complex but still it captures the main battery nonlinear characteristics. The reaction at the electrode involves electrons v^-, oxidized species O and reduced species R [3] :

$$O + v^- \rightarrow R\ (cathode)$$

Equation 8

$$R \rightarrow O + v^-\ (anode)$$

The electro-active species are uniformly distributed in the electrolyte when no load is connected (Figure 13a). When a load is connected and the electrons flow is established, the number of species near the electrode starts to decrease due to the electrochemical reaction and it creates a non-zero concentration gradient across the electrolyte (Figure 13b). When the load is switched off, the battery will start to recover as the concentration near the electrode surface will start to increase due to diffusion till the concentration gradient becomes zero again. The electro-active species concentration in the electrolyte will be less than the initial value though they are now uniformly distributed in the electrolyte (Figure 13c). The cathode reaction can no longer take place when the O concentration near it drops below a certain level (Figure 13d). Also the anode reaction cannot take place when the R concentration drops below a certain level. The model assumes that both the anode and cathode have

the same behavior to simplify the analysis and in the same time does not impair the accuracy of the lifetime prediction [3]. The time to failure is that when the reaction can no longer take place at the electrode.

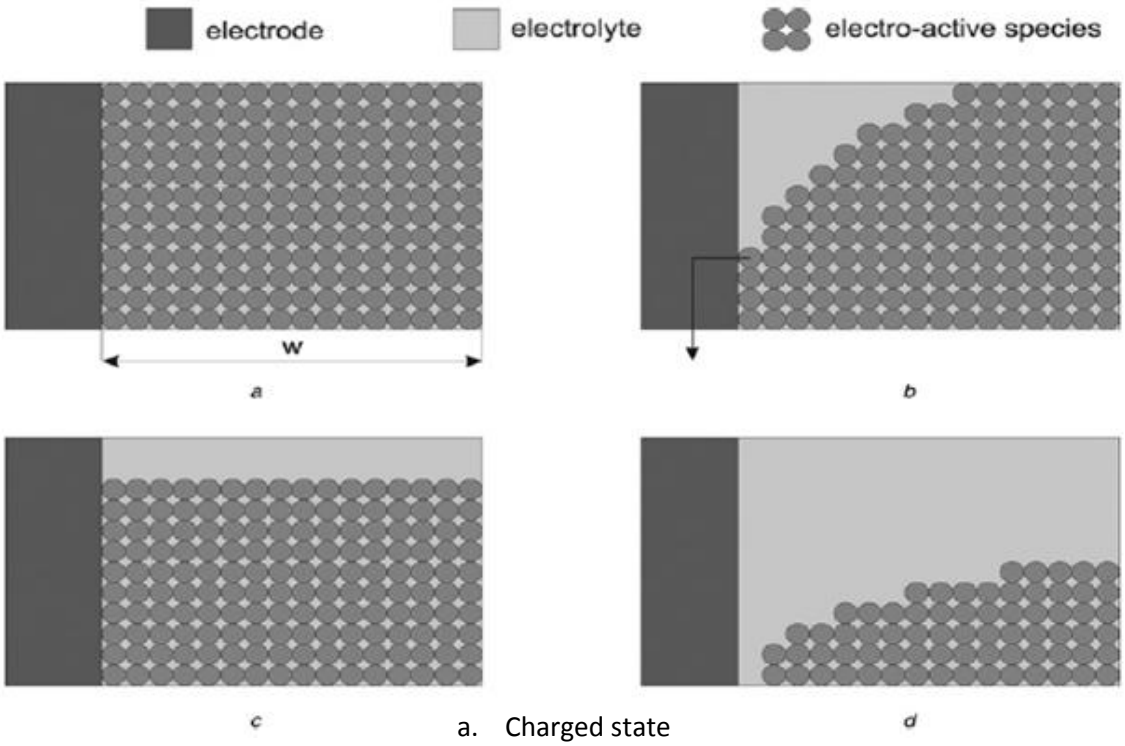

a. Charged state
b. Before recovery
c. After recovery
d. Discharged State

Figure 13: Physical Picture of Rakhmatov Diffusion Model [1]

The concentration of the electro-active species at time t and distance x Ɛ [0, w] is denoted by C(x,t). For the full battery the concentration is constant over the length of the electrolyte: C(x, 0) = C*, x Ɛ [0, w], where C* is the initial concentration and $\rho(t) = 1 - (\frac{C(0,t)}{C^*})$. The battery is considered empty when C (0, t) drops below the cutoff level C_{cutoff}. To calculate the lifetime of the battery in one cycle, an analytical expression for $\rho(t)$ needs to be found.

The evolution of the concentration is described by Fick's law [3]:

$$\begin{cases} -J(x,t) = D\,\frac{\partial C(x,t)}{\partial x} \\ \frac{\partial C(x,t)}{\partial t} = D\,\frac{\partial^2 C(x,t)}{\partial^2 x} \end{cases}$$

Equation 9

Where J (x, t) is the flux of the electro-active species at time *t* and distance *x* from the electrode, and *D* is the diffusion coefficient. The flux at the electrode surface (x = 0) is proportional to the current [*i(t)*]. The flux on the other side of the diffusion region (x = w) equals zero. This leads to the following boundary conditions [3]:

$$\begin{cases} D \left.\frac{\partial C(x,t)}{\partial x}\right| (x = 0) = \frac{i(t)}{vFA} \\ D \left.\frac{\partial C(x,t)}{\partial x}\right| (x = w) = 0 \end{cases}$$ **Equation 10**

Where A is the area of the electrode surface, F is Faraday's constant and *v* is the number of electrons involved in the electrochemical reaction at the electrode surface. It is possible to obtain an analytical solution for the set of partial differential equations together with the initial condition and the boundary conditions using Laplace transforms. From that solution one can obtain the following solution [3]:

$$\rho(t) = \frac{1}{vFAwC^*}\left[\int_0^t i(\tau)d\tau + \lim_{\varepsilon\to 0^+} 2\sum_{m=1}^{\infty}\int_0^{t-E} i(\tau)\, e^{-\frac{\pi^2 D(t-\tau)m^2}{w^2}} d\tau\right]$$ **Equation 11**

Letting $\beta = \left(\frac{\pi\sqrt{D}}{w}\right)$ and $\alpha = vFAwC^*\rho(L)$, then the following equation relates the load, the time to failure and the two battery parameters β and α:

$$\alpha = \int_0^L i(\tau)\, d\tau + 2\sum_{m=1}^{\infty}\int_0^L i(\tau)\, e^{-\beta^2 m^2 (L-\tau)}\, d\tau$$ **Equation 12**

The battery is empty when the apparent charge lost α is equal to the battery capacity. Rakhmatov et al. then tries to simplify the above equation by solving for two general cases: the constant load case and the variable load case. For the constant case, i(t) can be replaced by constant I, and the equation becomes:

$$\alpha = IL\left[1 + 2\sum_{m=1}^{\infty}\frac{1-e^{-\beta^2 m^2 L}}{\beta^2 m^2 L}\right]$$ **Equation 13**

And for the variable load case, they assumed that the current will be approximated by step function in form of:

$$i(t) \approx \sum_{k=0}^{N-1} I_k[U(t-t_k) - U(t-t_{k+1})]$$ **Equation 14**

And then the model equation becomes:

$$\alpha \approx \sum_{k=0}^{N-1} I_k F(L, t_k, t_{k+1}, \beta)$$ **Equation 15**

Where

$$F(L, t_k, t_{k+1}, \beta) = t_{k+1} - t_k + 2\sum_{m=1}^{\infty} \frac{e^{-\beta^2 m^2 (L - t_{k+1})} - e^{-\beta^2 m^2 (L - t_k)}}{\beta^2 m^2}$$

It was proven in [1] that Rakhmatov's Diffusion Model is a continuous version of the KiBaM. KiBaM is considered to be a first order approximation of the Diffusion Model. The Diffusion model can be used for any type of loads and it captures the nonlinear characteristics of the battery. It can predict the lifetime with maximum error of 4% [3].

3. Battery Management and Optimization

Battery managing and optimizing the battery lifetime is one of the most important research topics in the field of battery operated handheld electronic devices. There are a lot of techniques and approaches to manage the battery system. One approach of managing the battery is to scale the supply voltage of the system [2]. V_{dd} is selected to find a tradeoff between the battery capacity and performance. The purpose is to optimize the battery discharge delay product, which is the product of the actual charge and the delay of the circuit for a given task [2]. In order to minimize the battery discharge delay product, a certain V_{dd} value is needed to be found. This technique does not aim at modifying the current discharge profile shape. Selecting a constant supply voltage to optimize the battery discharge delay product can be done if the current discharge profile of a given circuit can be statically determined [2].

Another technique for battery-driven system level power management is based on monitoring the state of charge of the battery and accordingly controlling the state of operation of the system [2]. For example, for a digital audio recorder that is battery operated, when the battery approaches a completely discharged state, the audio quality is degraded gracefully. This is done by monitoring the battery output voltage, and when it goes below a certain threshold, the quality of the device is degraded in order to extend the battery life. This technique is based on the rate capacity effect property of the battery [2].

There are also battery scheduling techniques that adapt a schedule for when to turn on/off the cells in order to enhance the lifetime [2]. There are two classes of battery scheduling techniques, the static scheduling that does not make use of any run time information, and the dynamic scheduling which is based on some aspects of the battery properties during run time [2].

As we mentioned earlier, the static scheduling technique does not make use of either the system discharge profile or the battery state of charge. Serial scheduling is one type of this technique where all batteries are discharged one after the other [2]. Another approach is random scheduling, where a cell is chosen at random at each discharge interval and it is discharged for a fixed time. Another static scheduling approach is the Round-Robin Scheduling where a battery cell is chosen in round robin method for each discharge

interval. In comparison to the serial scheduling approach, random scheduling and round-robin scheduling are better in terms of system lifetime because they allow recovery time for the cells during idle periods of time. A selector circuit to switch between the different cells is required in both techniques. It was found that the higher the switching frequency, the higher the improvements in the battery capacity but this happens with diminishing returns due to the large time constraints related to the batteries and the energy consumed in the switching circuit [2].

A modified round robin technique takes into account the battery output voltage where the round robin is used until the output voltage of one or more batteries go below a certain threshold [2]. When one or more battery voltage is below the threshold, they are disconnected from the scheme and they are given some idle time for recovery. When they recover enough charge, they are put back to the round robin scheme. When all the batteries voltage is below the threshold, they are then all discharged in the fixed round robin scheme. In another approach, the round robin fashion is used but with a variable discharge interval depending on the state of charge of the battery [2].

Jiong et al. proposed two battery aware scheduling techniques. The first aims at maximizing the utilization of the battery capacity by optimizing the discharge power profile. The second one aims at reducing the discharge power consumed and to flatten the discharge power profile [26]. It is based on variable voltage scheduling via efficient slack time re-allocation. This technique is suitable for systems that have voltage scalable processing elements. Those techniques were achievable via developing an evaluation metric that is aware of the battery discharge power profile. They showed that 29% increase in battery lifetime can be achieved by optimizing the power discharge profile. It was also found that the variable voltage scheduling scheme with slack allocation increases the lifetime by 76% vs. the non-scalable scheme [26]. They have used the fact that reducing the average discharge current increases the lifetime and they achieved this through voltage scaling and processing elements shutoff. Performing schedule transformations that does not violate the original schedule constraints helps in optimizing the discharge current profile and therefore improve the utilized battery capacity [26].

Rakhmatov et al. addressed the task sequencing problem with and without voltage scaling in order to increase the battery lifetime by shaping the discharge profile. They used the diffusion model developed earlier by them as a basis of a battery aware cost function to develop algorithms for the task sequencing. They also utilized the insertion of recovery periods to increase the lifetime and voltage scaling for delay slack distribution [27].

Benini et al. investigated using battery related information like the output voltage, depth of discharge or state of charge to perform dynamic battery scheduling. They did not schedule the battery cells to operate each in a unique time slice, but depending on the battery information observed, the battery will be discharged for a different amount of time. They assumed that the dynamic scheduling provide better opportunity to enhance the battery lifetime than static scheduling as it can utilize the idle times during which charge recovery happens [28].

Another approach for managing a battery system is introduced by Suman Mandal et al. They proposed a new battery system, IntelBatt. It aims at saving more energy through introducing a new intelligent battery cell array (IBCA) manager [29]. The IBCA manager monitors the cells status and optimizes its capacity through cell scheduling. IntelBatt can be used for any battery operated electronic equipment since it does not assume any equipment knowledge. It consists of three main components: cell array, cell switching circuit and the IBCA manager (Figure 14). The cell array is a collection of banks, where inside each bank there are one or more cells in parallel connection. The cell switching circuit (CSC) connects the battery's main terminals to the cell array. The CSC circuit, as shown in Figure 15, consists of a matrix of two switches. A control signal can turn the switches on/off such that any cell can be connected to any bank. Based on a code word, the IBCA manager can configure the cell switching circuit. The cell scheduling algorithm is based on the discharge cycle length and the battery life. Given the load current I_t and $V_{cell,i}$, the most efficient cell configuration should meet the following conditions: For each cell k, $I_k < I_k^{max}$ and $V_{cell,k} > V_{cell,\,k}^{cutoff}$. The minimum voltage needed in a bank is given by V_{min} . I^{max} is the current that can be drawn from the cell safely without causing a short circuit. V^{cutoff} is the cell discharge limit. At least one cell in each bank is necessary

to maintain the output voltage level. If there are *n* available cells and *k* banks, cell selection can be formulated as the determination of a subset of all possible *k* clusters [29].

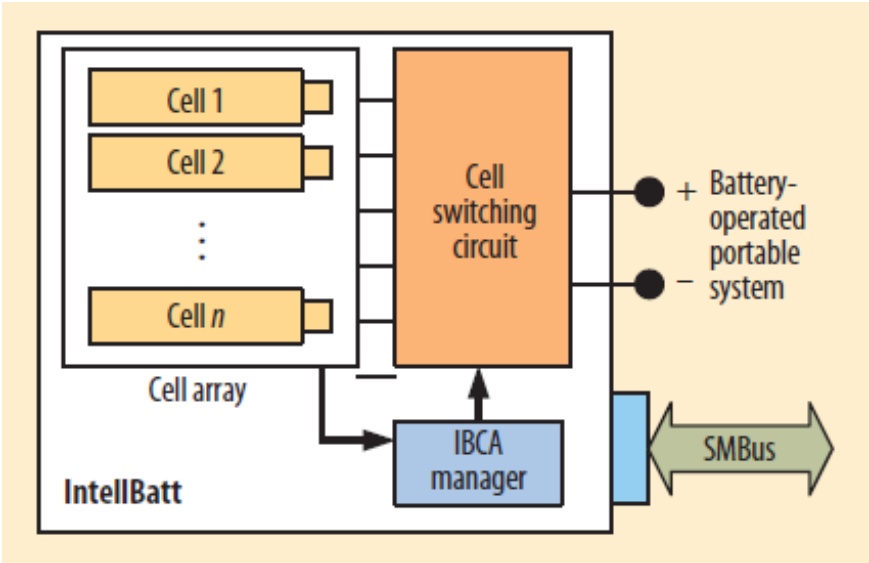

Figure 14: IntelBatt Architecture [29]

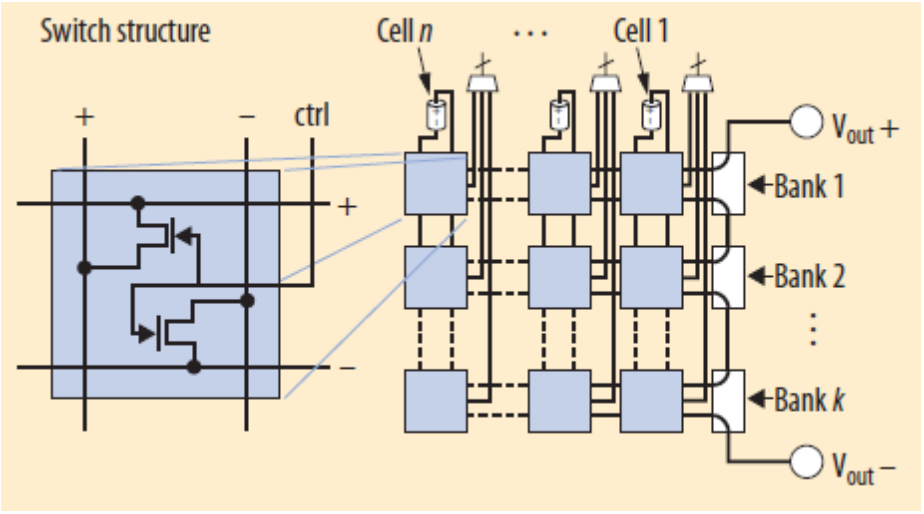

Figure 15: Cell Switching Circuit Design [29]

II. LITHIUM-ION BATTERY STUDY

The previous discussion indicates that understanding the nonlinear battery properties is very important in order to be able to model and optimize a battery system. This research aims at studying the lithium ion battery system and understands how the battery system can be optimized in order to achieve better lifetime of the cell. Both single cell and multi-cell systems will be studied. In this chapter and the coming ones, we will study the behavior of the lithium ion battery under various workloads. We will try to understand how it behaves and what affects its behavior. We are going to use Rakhmatov diffusion battery model to simulate the battery in SPICE simulator. Instead of using the two cases for constant and variable loads that Rakhmatov used, we are going to use the very general case in equation 12 to run our simulations. This will allow us to not only simulate constant and variable step function loads, but to simulate any variable load of any profile. In order to be able to use a SPICE simulator to predict the lifetime of the battery without having to use the complex algorithm developed by Rakhmatov, we are going to put equation 12 in another form.

$$\alpha = \int_0^L i(\tau)\,d\tau + 2\sum_{m=1}^{\infty}\int_0^L i(\tau)\,e^{-\beta^2 m^2 (L-\tau)}\,d\tau \qquad \text{Equation 12 revisited}$$

Let's consider the first term $\int_0^L i(\tau)\,d\tau$: it corresponds to a perfectly linear battery where the lifetime is the capacity divided by the constant current $L = \alpha/I_{const}$ (or more generally the integral of the current) like Peukert's law. The second term of the equation represents the battery nonlinearity as derived from Rakhmatov model. Now since L (lifetime) is in the exponential form, then solving the equation becomes very complex. So we will find L by solving the integral at each time step (assuming L= const = t enabling us to take it outside the integration). Then we solve the integration at each time step till we reach that the R.H.S is equal to α. At time t = 0, the R.H.S of the equation is equal to zero, where at t = L, the R.H.S is equal to α which means that the battery is fully discharged. Thus we can put the equation in the following form to represent the battery state of charge SOC:

$$SOC(\%) = 100 - 100 * \frac{(\int_0^L i(\tau)d\tau + 2\sum_{m=1}^{10}\int_0^L i(\tau)e^{-\beta^2 m^2(L-\tau)}d\tau)}{\alpha}$$ **Equation 16**

When SOC reaches zero, then the battery reaches the end of the lifetime for this discharging cycle. Notice that we used also the first ten terms of the summation as proved before to be sufficient and good approximation. At each time step, we will assume that L = t and thus it will become a constant value at each step, so we will take it out of the integral and the equation will then be:

$$SOC(\%) = 100 - 100 * \frac{(\int_0^L i(\tau)d\tau + 2\sum_{m=1}^{10} e^{-\beta^2 m^2 L}\int_0^L i(\tau)e^{\beta^2 m^2 \tau}d\tau)}{\alpha}$$ **Equation 17**

This equation can be easily solved in a SPICE simulator. When solving it, we had a problem with the exponential blow up limit as its value built up rapidly, so we applied a correction factor to decrease the exponential value without affecting the final result of the SOC.

$$SOC(\%) = 100 - 100 * \frac{(\int_0^L i(\tau)d\tau + 2\sum_{m=1}^{10} e^{CF-\beta^2 m^2 L}\int_0^L i(\tau)e^{\beta^2 m^2 \tau - CF}d\tau)}{\alpha}$$ **Equation 18**

Where CF is the Correction Factor and it will be adjusted when simulating to adjust the exponential value. This form of the equation is general for any current profile and will be used in the following studies. We used the least mean square estimation method in order to obtain the two battery parameters α and β. We used the 10 workloads from [3] that are collected from experimental data in order to get the α and β values. The details are shown in appendix A. We got $\alpha = 2418.49$ and $\beta = 0.036$.

We will first simulate using equation 18 to show the nonlinear behavior of the battery that this model is able to detect. Figure 16 shows the simulation of two batteries with a pulsed discharge current as the load, one of the batteries exhibits the nonlinear battery characteristics and the other does not.

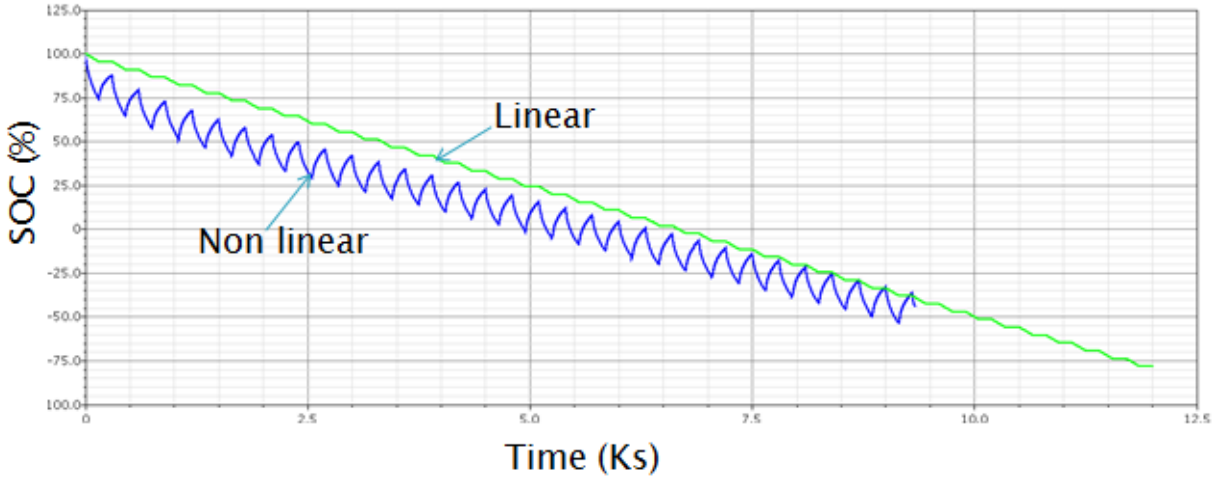

Figure 16: Nonlinear Discharge vs. Linear Discharge

Figure 17 is a closer look at the above simulation results. In the case of the nonlinear discharge, recovery takes place when the battery is idle. While in the linear discharge case, no recovery is taking place. Also it is noticed that the nonlinear battery exhibits nonlinear discharge curve, while the linear battery has a linear discharge curve.

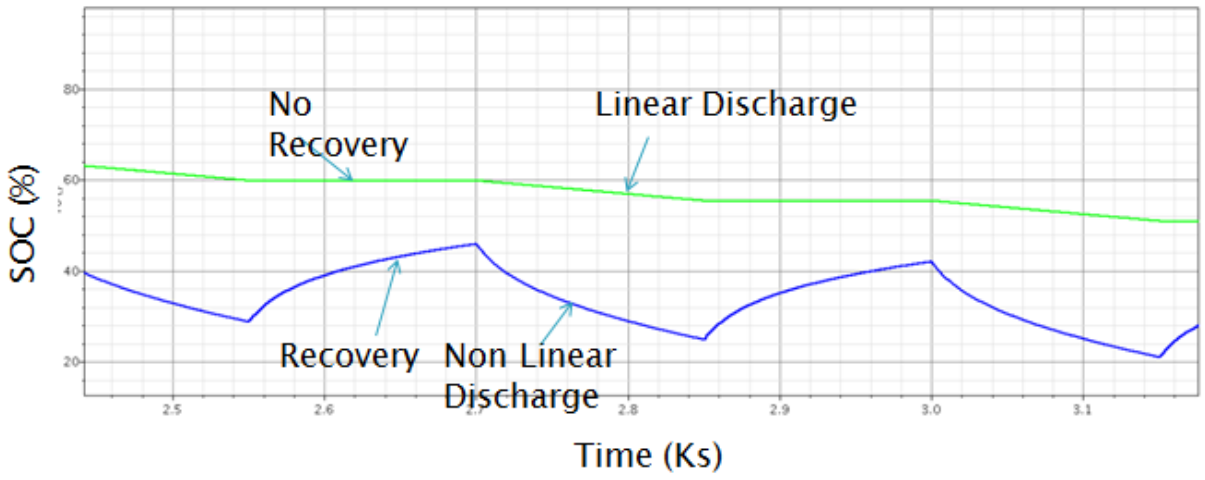

Figure 17: Nonlinear Discharge vs. Linear Discharge - 2nd. Curve

III. PROPOSED HYBRID BATTERY MODEL

In this chapter, we propose a new hybrid battery model that takes care of the battery nonlinearity (the recovery effect and the rate capacity effect) together with the electric circuit characteristics. This model is a hybrid model that combines the electric circuit model by Min Chen et al. with Rakhmatov analytical diffusion model. Min Chen's electric model (Figure 6) made the RC network parameters function of the SOC as follows [5]:

$$V_{OC}(SOC) = -a_1.e^{-a_2.SOC} + a_3 + a_4.SOC - a_5.SOC^2 + a_6.SOC^3 \quad \text{Equation 19}$$

$$R_{series}(SOC) = b_1.e^{-b_2.SOC} + b_3 \quad \text{Equation 20}$$

$$R_{Transient\_S}(SOC) = c_1.e^{-c_2.SOC} + c_3 \quad \text{Equation 21}$$

$$C_{Transient\_S}(SOC) = -d_1.e^{-d_2.SOC} + d_3 \quad \text{Equation 22}$$

$$R_{Transient\_L}(SOC) = f_1.e^{-f_2.SOC} + f_3 \quad \text{Equation 23}$$

$$C_{Transient\_L}(SOC) = -g_1.e^{-g_2.SOC} + g_3 \quad \text{Equation 24}$$

Where the coefficients of the exponentials and the other constants can be determined from experiments that measure the V_{OC} and the RC network parameters [5]. The value of the SOC in the equations would be determined with the value of $C_{capacity}$ (Figure 6). In this model, $C_{capacity}$ is assumed to be a constant value which was shown by our previous analysis that it is not true. The battery would have different capacities depending on the load profile due to its nonlinearity. So assuming $C_{capacity}$ to be constant will ignore the battery nonlinearity and will not take into account the recovery effect. So we propose to introduce a new equation taken from the diffusion model to the above electric model to take this into account. Since that V_{SOC} across the $C_{capacity}$ varies from 0 to 1, where 0 is fully discharged and 1 is fully charged, then we can remove the $C_{capacity}$, and calculate the V_{SOC} from the SOC equation we got in the previous chapter:

$$SOC(\%) = 100 - 100 * \frac{\left(\int_0^L i(\tau)d\tau + 2\sum_{m=1}^{10} e^{CF-\beta^2 m^2 L}\int_0^L i(\tau)e^{\beta^2 m^2 \tau - CF}d\tau\right)}{\alpha} \quad \text{Equation 25}$$

Then

$$V_{SOC} = SOC/100$$ **Equation 26**

So we will introduce the two parameters: α and β to the electric model. Now this model will take into account the rate capacity effect and the recovery effect.

The new proposed hybrid model is shown in Figure 18.

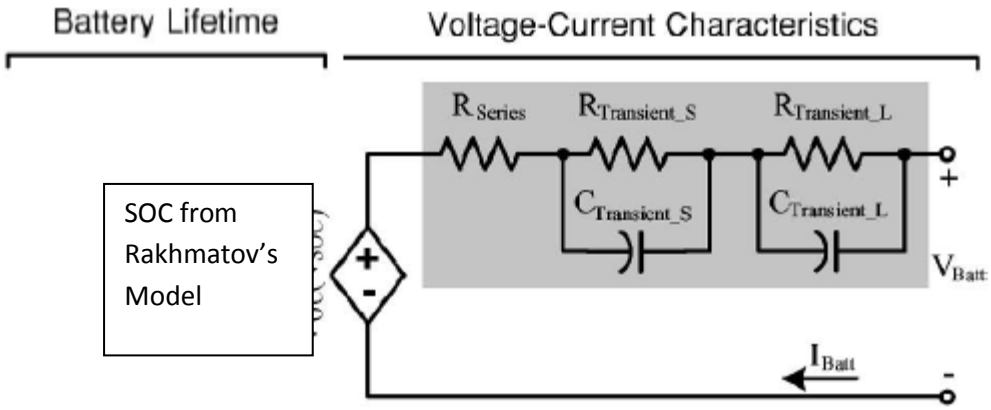

Figure 18: New Proposed Hybrid Model

And below are the new hybrid model equations:

$$V_{SOC} = 1 - \left(\frac{\int_0^L i(\tau)d\tau + 2\sum_{m=1}^{10} e^{CF-\beta^2 m^2 L}\int_0^L i(\tau)e^{\beta^2 m^2 \tau - CF}d\tau}{\alpha}\right)$$ **Equation 27**

$$V_{OC}(SOC) = -a_1.e^{-a_2.SOC} + a_3 + a_4.SOC - a_5.SOC^2 + a_6.SOC^3$$ **Equation 28**

$$R_{series}(SOC) = b_1.e^{-b_2.SOC} + b_3$$ **Equation 29**

$$R_{Transient\_S}(SOC) = c_1.e^{-c_2.SOC} + c_3$$ **Equation 30**

$$C_{Transient\_S}(SOC) = -d_1.e^{-d_2.SOC} + d_3$$ **Equation 31**

$$R_{Transient\_L}(SOC) = f_1.e^{-f_2.SOC} + f_3$$ **Equation 32**

$$C_{Transient\_L}(SOC) = -g_1.e^{-g_2.SOC} + g_3$$ **Equation 33**

Table 2 shows the parameters used to simulate this model. The parameters a1 through g3 are taken from Min Chen's electric circuit model in order to be able to compare against it.

Table 2: Hybrid Battery Model Parameters

a1	-1.031	b1	0.1562	d1	-752.9	g1	-6056
a2	-35	b2	-24.37	d2	-13.51	g2	-27.12
a3	3.685	b3	0.07446	d3	703.6	g3	4475
a4	0.2156	c1	0.3208	f1	6.603	α	2418.499
a5	-0.1178	c2	-29.14	f2	-155.2	β	0.036
a6	0.3201	c3	0.04669	f3	0.04984		

The above model was simulated in Cadence (schematics are included in appendix B). Figure 19 shows the simulation results of our hybrid model vs. the electric circuit model. We used a constant current of 100mA to discharge the battery. We found that the battery SOC is linear as expected in the electrical model while the nonlinear behavior was captured by our hybrid model as expected. On the other hand, the nonlinear output voltage was captured with our model and it is following the output voltage of the electric circuit model. The V_{SOC} of our model is an exact match for V_{SOC} calculated from Rakhmatov's model.

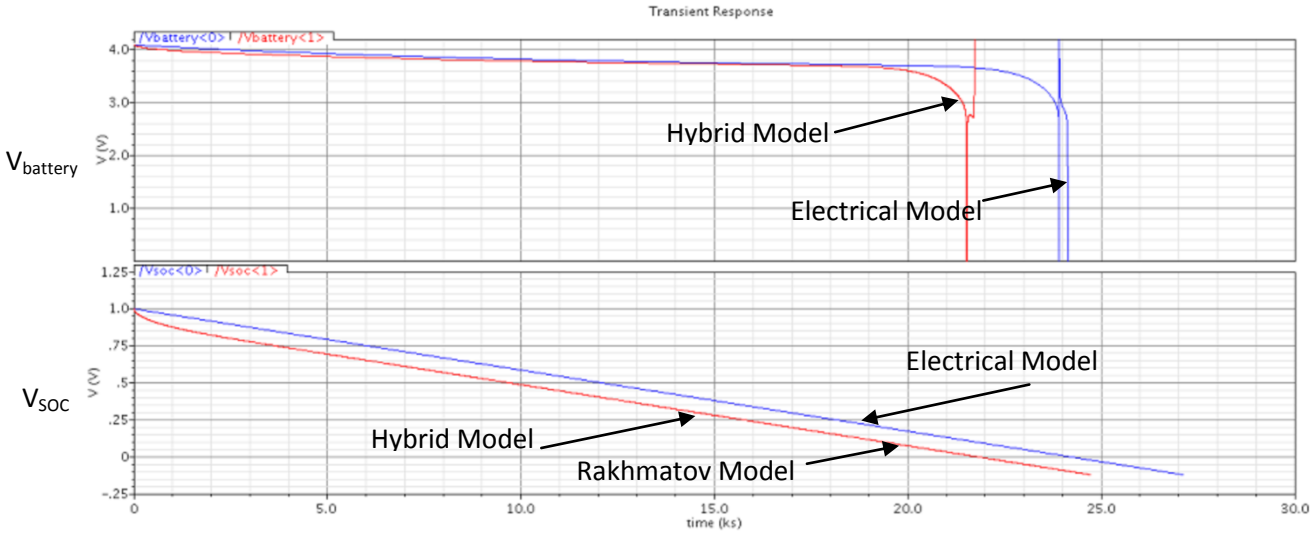

Figure 19: Hybrid Model vs. Electric Circuit Model

Table 3 shows the run time taken by the hybrid model against each of the linear battery model, the Rakhmatov Diffusion model and the Electrical model. Our model takes reasonable simulation time compared to the other models. It is taking slightly more

time than the other models but that is due to the more accuracy and features that are taken into account.

Table 3: Comparison of Simulation Time of Different Battery Models

Model	Linear	Electrical	Diffusion	Hybrid
Simulation Time (sec)	2.3	6.6	2.3	9.2
Post Processing Time (sec)	1.1	1.0	5.1	6.5

IV. LITHIUM ION BATTERY SIMULATION RESULTS

First, using the same battery parameters used by Rakhmatov (i.e. same α and β). We simulated the 22 variable current profiles as shown in Table 4. Those are the loads simulated by Rakhmatov. We verified that our general form of Equation 18 is valid. The table includes the profile number in column 1, the current value in column 2 and the corresponding duration time in column 3. For example, C1 will have current of 628mA from time 0 to time 19.5s, then it will be idle from 19.5s to 26s, then it will have again current of 628mA from time 26s till the battery is empty. For profiles with periodic loads the first period is enclosed between brackets and then the bracket is followed with the number of repetitions of the period. For example in C13, the enclosed period will be repeated for 5 times. For the time set, the brackets are followed with the repetition number as well as the total duration of one period (i.e. C13: the total period duration is 22.5 minutes). For the last case, C22, the current is incrementing by 5 mA each minute till the battery is completely discharged.

Table 4: Variable Current Load Sets [3]

Profile Number	Current Value set (mA)	Timing set (min)
C1	628,0,628	0, 19.5, 26
C2	494.7,0,494.7	0, 31, 41.3
C3	425.6,0,425.6	0, 41, 54.6
C4	292.3,0,292.3	0, 74.6, 99.5
C5	222.7,0,222.7	0, 105.7, 140.9
C6	628,0,628	0, 19.5, 29.9
C7	628,0,628	0, 19.5, 22.1
C8	628,0,628	0, 23.4, 29.9
C9	628,0,628	0, 15.6, 22.1
C10	300, 628, 494.7, 252.3, 234.1, 137.9, 113.9, 265.6	0, 0.5, 5.5, 10.5, 35.5, 60.5, 85.5, 110.5
C11	300, 113.9, 137.9, 234.1, 242.3, 494.7, 628. 265.6	0, 0.5, 25.5, 50.5, 75.5, 100.5, 105.5, 110.5
C12	300, 113.9, 137.9, 234.1, 242.3, 494.7,0, 300, 628, 265.6	0, 0.5, 25.5, 50.5, 75.5, 100.5, 105.5, 130.5, 131, 136
C13	300, (628, 494.7, 252.3, 234.1, 137.9, 113.9)5, 256.6	0, (0.5, 1.5, 2.5, 7.5, 12.5, 17.5)(5, 22.5), 110.5
C14	300, (113.9, 137.9, 234.1, 252.3, 494.7, 628)5, 256.6	0, (0.5,5.5, 10.5, 15.5, 20.5, 21.5)(5, 22.5), 110.5
C15	222.7, 204.5, 108.3, 84.3, 222.7	0, 50, 100, 150, 200
C16	84.3, 108.3, 204.5, 222.7, 222.7	0, 50, 100, 150, 200
C17	84.3, 108.3, 204.5, 0, 222.7, 222.7	0, 50, 100, 150, 200, 250
C18	(84.3, 108.3, 204.5, 222.7)10, 222.7	(0, 5, 10, 15) (10,20), 200
C19	(75.5, 94.9, 204.5, 222.7)10, 222.7	(0, 5, 10, 15) (10,20), 200
C20	(494.7, 628) inf	(0,1) (inf, 2)
C21	(494.7, 628, 57.6) inf	(0, 1, 2) (inf, 3)
C22	(5, 10, 15, …)	(0, 1, 2, …)

The results of our SPICE simulations are shown against those obtained from Rakhmatov as well against Dualfoil results in Table 5.

Table 5: Lifetime Values Obtained from SPICE Simulation

Profile Number	LT_DualFoil (min)	LT_Rakhmatov (min)	LT_Equation18 (min)
C1	36.4	36.2	36.8
C2	57.2	55.8	56.6
C3	74.2	71.9	72.7
C4	128.1	124.9	125.8
C5	178.5	176.7	177.7
C6	41.5	41.0	41.6
C7	30.6	30.8	31.6
C8	37.0	37.4	38.0
C9	35.4	35.2	36.0
C10	135.2	132.6	133.6
C11	108.8	107.4	108.0
C12	159.0	155.4	157.6
C13	133.8	131.7	131.7
C14	132.9	129.7	129.7
C15	207.6	209.2	209.7
C16	202.4	200.7	202.0
C17	253.8	251.2	252.3
C18	204.6	204.6	205.3
C19	209.4	208.7	209.7
C20	31.7	33.2	33.6
C21	55.9	55.9	58.6
C22	97.5	94.5	94.5

We show the maximum and average differences between our simulations and Dual foil ones, and those obtained by Rakhmatov and Dual foil. In Table 6, it is shown that with our SPICE simulations, since using the general case and not the approximated equation as used by Rakhmatov, we have less maximum and average differences from the Dual foil results than Rakhmatov's.

Table 6: Simulation Delta From DualFoil

Profile Number	Delta Rakhmatov* (min)	Delta Equation18** (min)
C1	0.20	0.35
C2	1.40	0.60
C3	2.30	1.53
C4	3.20	2.30
C5	1.80	0.83
C6	0.50	0.12
C7	0.20	0.97
C8	0.40	1.03
C9	0.20	0.55
C10	2.60	1.63
C11	1.40	0.80
C12	3.60	1.45
C13	2.10	2.10
C14	3.20	3.20
C15	1.60	2.07
C16	1.70	0.40
C17	2.60	1.47
C18	0.00	0.73
C19	0.70	0.27
C20	1.50	1.85
C21	0.00	2.65
C22	3.00	3.00
average delta (min)	1.55	1.36
max delta (min)	3.60	3.20

**The difference in minutes between Lifetimes obtained from Rakhmatov's model and results from DualFoil.*

***The difference in minutes between Lifetimes obtained from our simulations and results from DualFoil.*

From those simulations, it is observed that:

- The more the depth of discharge, the less lifetime of the battery.
- Idle periods allow recovery of the battery charge.
- The slope of the recovery is not linearly proportional with the idle time. The recovery has more weight at the beginning of the rest period as shown in Figure 20.

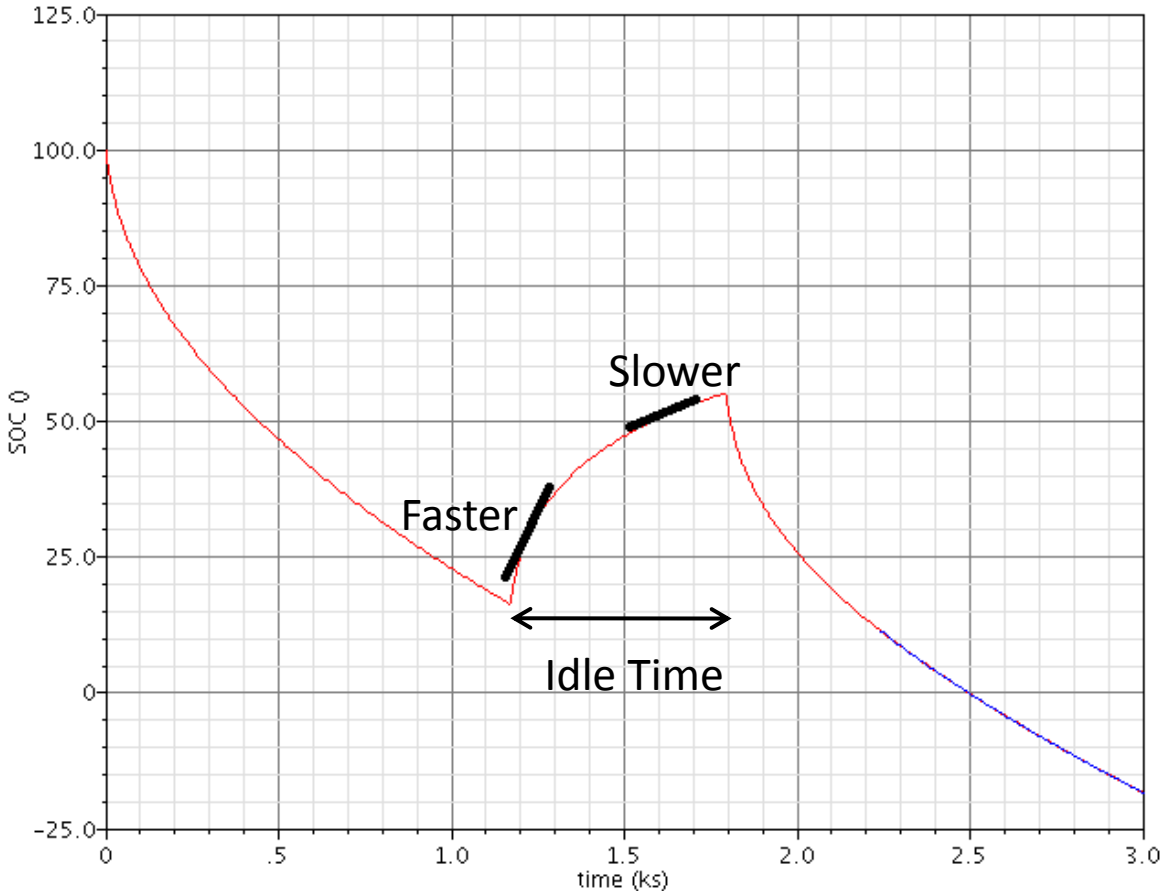

Figure 20: Slope of Recovery

In Table 7, for each of the profiles [C1-C22], we calculated the average current for each one and simulated the battery with it as a load. The results are then compared against the original variable current profiles. The data are arranged from the highest average current to the lowest. It is observed that:

- The average current load always has better lifetime than the corresponding variable current profile.
- The lifetime increases as the average current load decreases.
- The more the depth of discharge, the less the battery lifetime.
- The battery capacity (Ampere-Hour) is not constant for the same battery. It depends on the current profile of the load. And it is not linearly proportional with the discharge current (Figure 21).
- The battery capacity (Ampere.Hour) consumed from the battery increases as the average current load decreases.

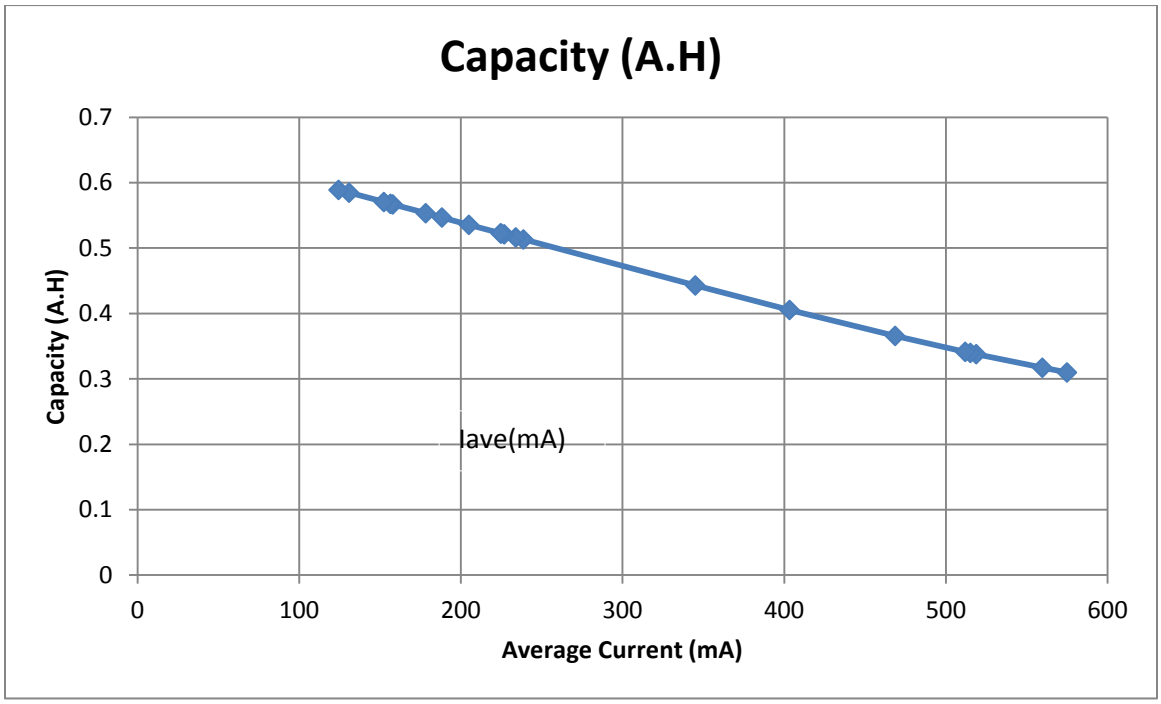

Figure 21: Capacity vs. Average Current

Table 7: Lifetime of Iaverage vs. Lifetime of Ivariable

Profile Number	Iave (mA)	LT_Ivar (min)	LT_Iave (min)	%LT inc	Capacity (A.H) = Iave*LT_Iave
C7	574.99	31.57	32.33	2.43	0.31
C20	559.74	33.55	33.98	1.29	0.32
C8	518.86	38.03	39.07	2.72	0.34
C1	515.24	36.75	39.57	7.66	0.34
C9	512.03	35.95	40.00	11.27	0.34
C6	468.70	41.62	46.82	12.49	0.37
C2	403.38	56.60	60.30	6.54	0.41
C3	345.10	72.67	77.00	5.96	0.44
C21	399.02	58.55	79.08	35.07	0.53
C22	238.76	94.50	128.97	36.47	0.51
C4	234.03	125.80	132.38	5.23	0.52
C10	226.91	133.57	137.78	3.16	0.52
C13	225.03	131.70	139.27	5.75	0.52
C14	224.62	129.70	139.58	7.62	0.52
C11	205.04	108.00	156.72	45.11	0.54
C12	188.36	157.55	174.17	10.55	0.55
C5	178.34	177.67	186.17	4.78	0.55
C15	157.93	209.67	215.33	2.70	0.57
C18	156.47	205.33	217.67	6.01	0.57
C19	152.46	209.67	224.50	7.07	0.57
C16	130.90	202.00	268.00	32.67	0.58
C17	124.43	252.33	284.00	12.55	0.59

Figure 22 below shows the simulation results for variable current loads in form of pulses but with different frequencies and with the same average current. The results are plotted against the results of the average current profile. T_p on the figure denotes the period of the current pulses. From these results, it is observed that:

- The highest frequency current profile (T_p = 1 sec) lies on the same curve of the average current profile.

- As the frequency increases, the variable current profile results in a very close lifetime as that of the average current profile (i.e. the savings are not significant).
- If we want to get benefit of the savings in the lifetime using average current profile, the savings will be more significant if the average current method is used on a macro scale level than on micro level of a processor for example, since on the micro scale, the frequency is very high and thus no significant savings can be achieved if an average current profile is used.

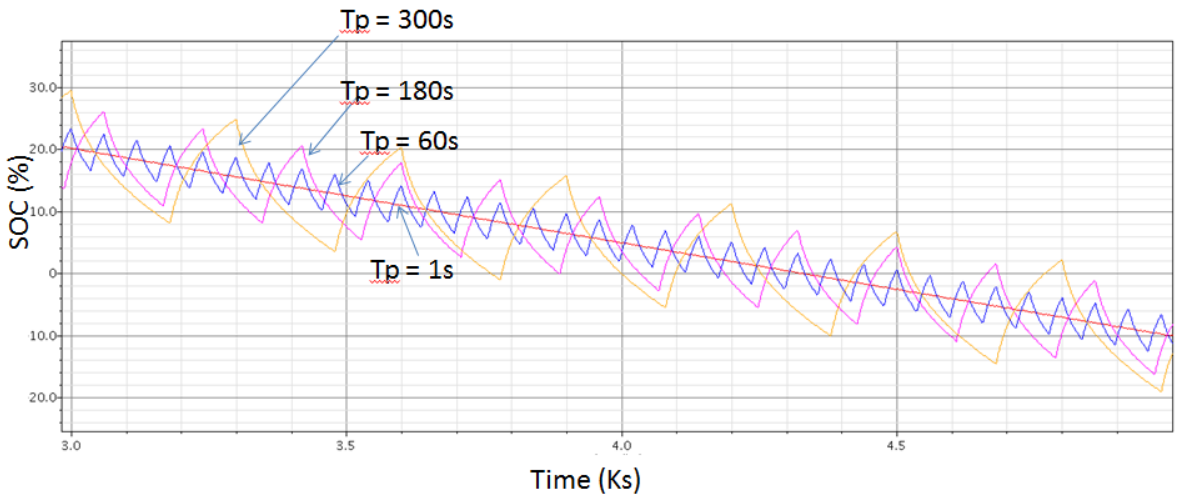

Figure 22: Simulated loads with Same Average Current but Different Frequencies

We studied further the savings that can be gained when using the average current profile. Different variable current profiles that have the same average current were simulated. We vary the variable profiles in two parameters: the period and the duty cycle while maintaining the same average current. For each set of loads that have the same average current: the ratio between the lifetime of the variable current load to the lifetime of the average current load are plotted in Figure 23 on the y-axis against the different duty cycles on the x-axis. It is found that the savings in lifetime increases when using an average current profile vs. a variable current profile as

- The duty cycle of the variable current profile decreases.
- The frequency of the variable current profile decreases.
- The average current of the variable profile increases.

Also, from the graph, it is clear that the average current profile is always giving better lifetime than the variable profile. 15%-60% savings in lifetime can be reached by using the average current profile.

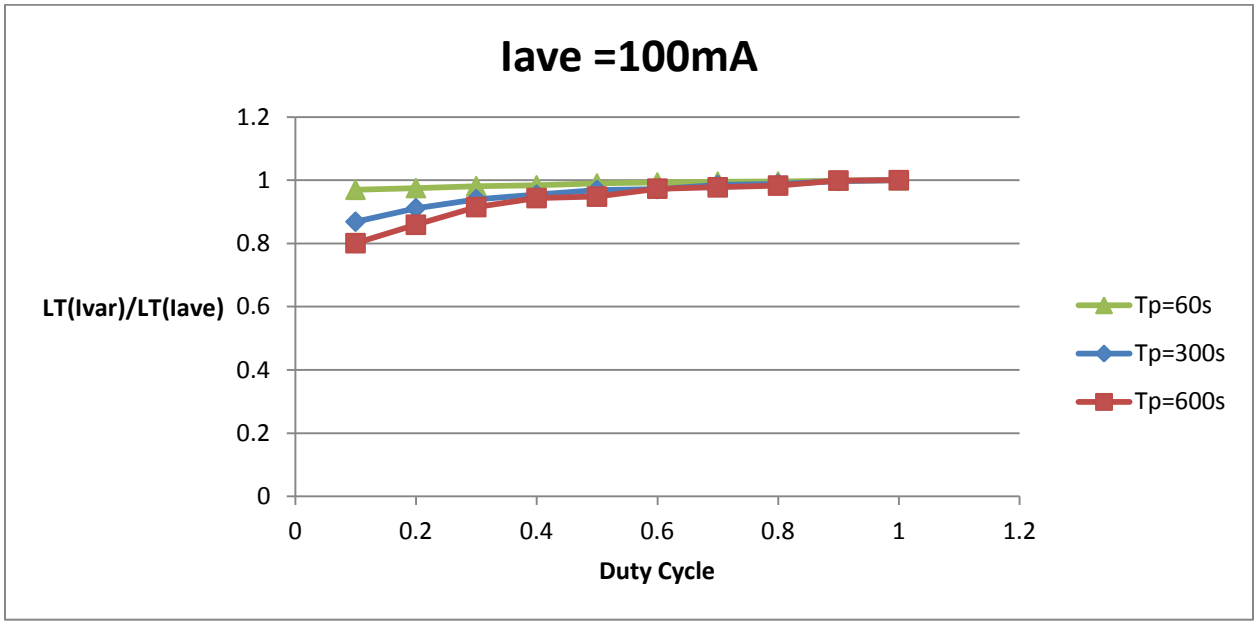

(a)

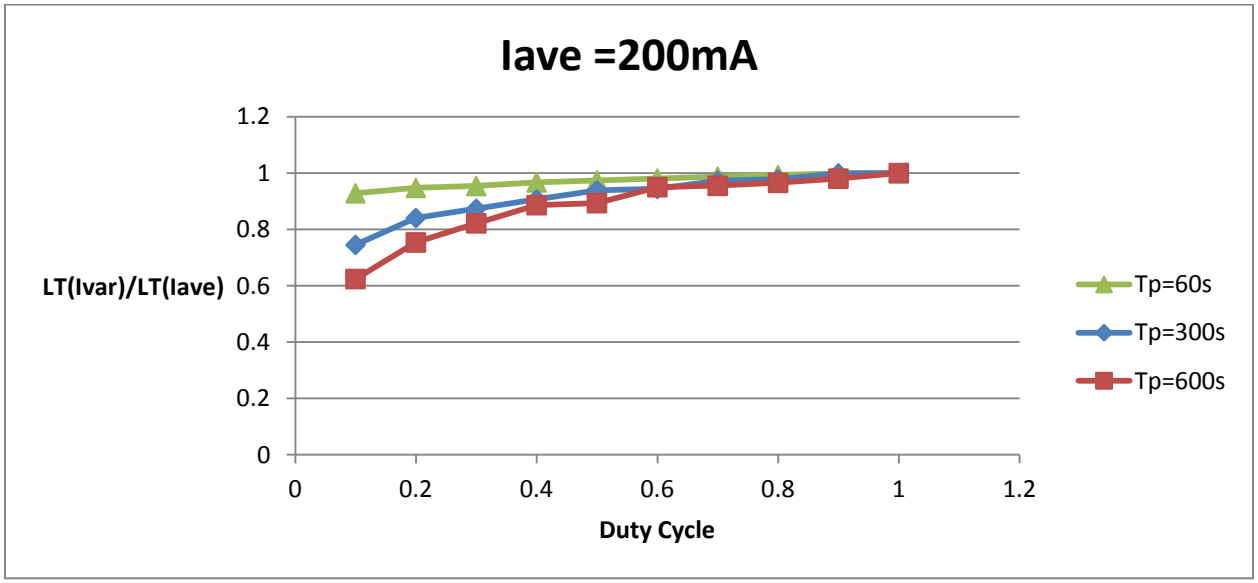

(b)

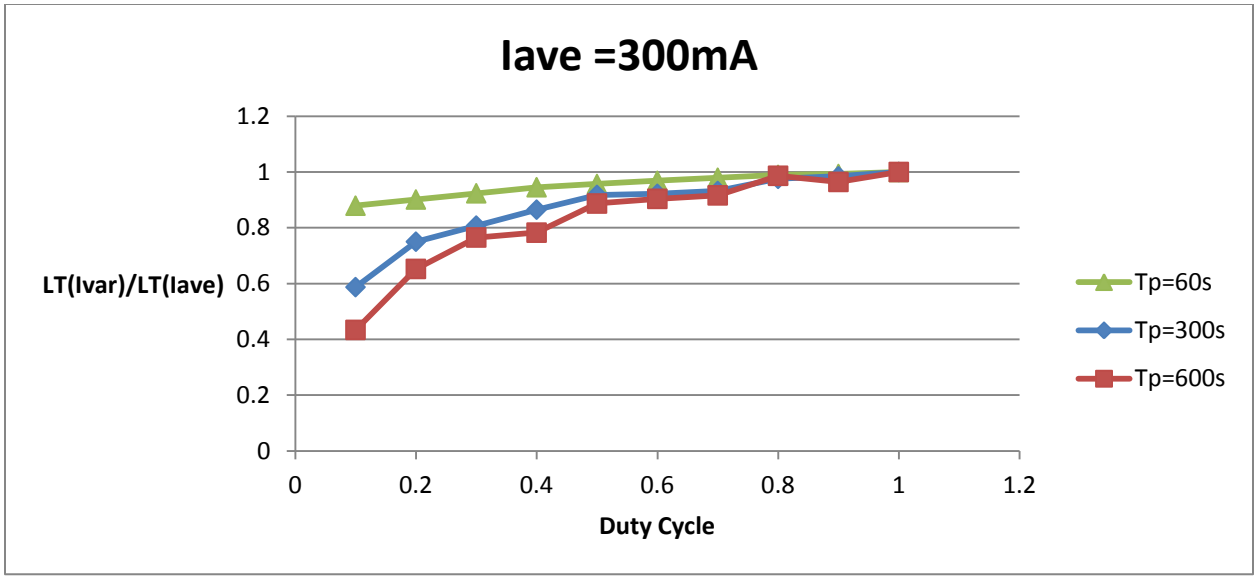

(c)

Figure 23: on the x-axis: ratio between Lifetime of the Variable Current Profile to Lifetime of the Average current, and on the y-axis: the duty cycle of the variable current profile. (a) Average current of the variable profiles = 100mA. (b)Average current of the variable profiles = 200mA. (c) Average current of the variable profiles = 300mA.

V. MULTI-CELL STUDY

In this section we will study the behavior of using multi cells of lithium ion battery. We will study the different cell configurations and how to optimize and manage the battery system. Table 8 shows the lifetime of using one cell, two cells in parallel and three cells in parallel. From the simulation results, it is shown that using two cells in parallel increases the lifetime by more than two times of using one cell. Same for the three cells, the lifetime of them is better by more than three times of using one cell. Figure 24 shows that the gain in the lifetime increases as the duty cycle increases and as the number of cells increases.

Table 8: Multi Cells in Parallel Configuration vs. Single Cell

Tp = 300s, Duty Cycle = 0.5					
I(mA)	LT_1_Cell(s)	LT_2_Cells(s)	LT_3_Cells(s)	ratio(2:1)	ratio(3:1)
200	21120	45383	69402	2.149	3.286
300	13020	29206	45395	2.243	3.487
600	4930	13016	20850	2.640	4.229
Tp = 300s, Duty Cycle = 0.8					
200	12500	27524	42760	2.202	3.421
300	7425	17566	27718	2.366	3.733
600	2544	7422	12489	2.917	4.909

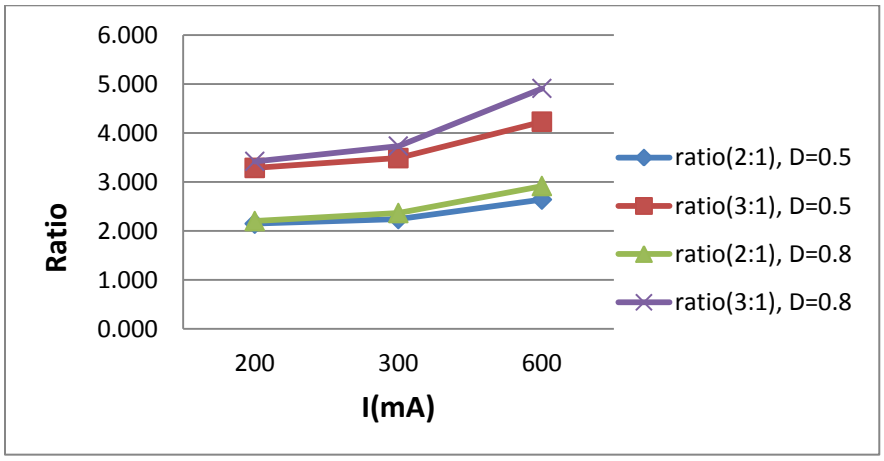

Figure 24: Multi Cells in Parallel Configuration vs. Single Cell

We had also simulated multi-cells system from two to nine cells in different configurations. Besides the parallel and serial configuration, we have added a new configuration to the comparison. The new configuration will be alternating between the different cells in the system, such that only once cell is on at a time, and the switching between the cells is done with a fixed period. We have used a constant current profile (I = 500mA) and we have varied the period by which the cells are on/off. Table 9 shows the comparison between the three configurations. From the table, we can observe that:

- As the number of cells increases, both the alternating and parallel configurations have better gains in lifetime over the serial configuration. The parallel configuration makes use of the rate capacity effect, i.e. the depth of discharge is decreased per cell when we add more cells to the configuration. The alternating configuration makes use of the recovery effect. The more we add cells, the more recovery time will be allowed per one cell.
- For the parallel configuration, the gain in lifetime saturates as we approach the seven cells system. As we increase the number of cells, depth of discharge will decrease per one cell, but as the current decreases beyond certain point, the slope of depth of discharge of the current profile becomes constant with respect to the battery capacity (Figure 25).
- For the alternating configuration, the gain in lifetime saturates as we approach the seven cells system as well. As we increase the number of cells, the recovery time (idle time) available for each cell increases. However, as shown before (Figure 20), the recovery is significant at the beginning of the idle period and then the gain from it becomes slower. Therefore, the recovery gained by adding more cells does not become as significant after seven cells (Figure 25)
- As we increase the period by which we switch the cells with (i.e. decreasing the frequency), the gain in the lifetime of the alternating approach decreases (but not with a significant value). This is due to the rate capacity effect: as the depth of discharge increases, the lifetime decreases.

Table 9: Comparison between Three Multi-Cell Configurations

Period = 60s					
Number of Cells	Serial Configuration LT	Alternating Configuration LT	Alternating Configuration LT : Serial Configuration LT	Parallel Configuration LT	Parallel Configuration LT : Serial Configuration LT
1	2500				
2	5000	7046	1.409	7271	1.454
3	7500	11718	1.562	12117	1.616
4	10000	16454	1.645	16951	1.695
5	12500	21192	1.695	21792	1.743
6	15000	25989	1.733	26631	1.775
7	17500	30780	1.759	31455	1.797
8	20000	35647	1.782	36300	1.815
9	22500	40280	1.790	41135	1.828
Period = 120s					
1	2500				
2	5000	6891	1.378	7271	1.454
3	7500	11438	1.525	12117	1.616
4	10000	16109	1.611	16951	1.695
5	12500	20784	1.663	21792	1.743
6	15000	25579	1.705	26631	1.775
7	17500	30325	1.733	31455	1.797
8	20000	35055	1.753	36300	1.815
9	22500	39760	1.767	41135	1.828
Period = 180s					
1	2500				
2	5000	6742	1.348	7271	1.454
3	7500	11216	1.495	12117	1.616
4	10000	15880	1.588	16951	1.695
5	12500	20552	1.644	21792	1.743
6	15000	25228	1.682	26631	1.775
7	17500	29904	1.709	31455	1.797
8	20000	34582	1.729	36300	1.815
9	22500	39320	1.748	41135	1.828

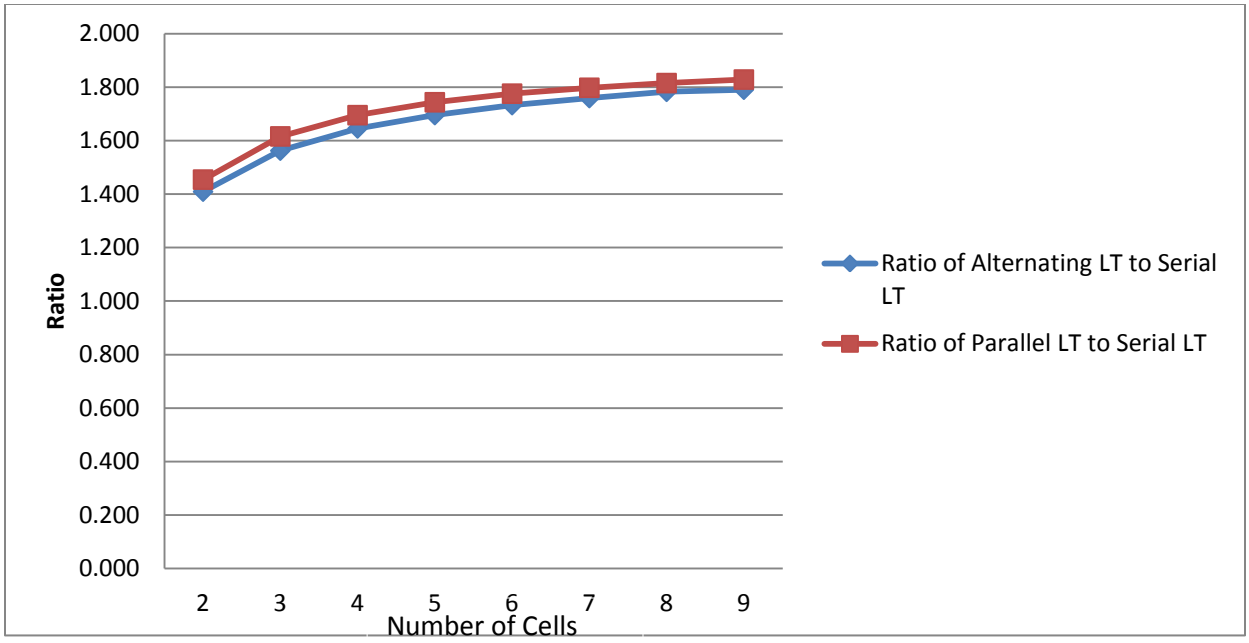

Figure 25: Lifetime Improvements over Using Serial Configuration

VI. CONCLUSION

The work presented here gives a good understanding of the nonlinear battery properties and how it affects its lifetime. It was shown that 15-60% of savings in the lifetime can be achieved if we used the average current profile instead of the variable current profile. It was also shown that the lifetime savings by using the average current are more significant on the macro scale level of the system and not on the micro scale. The nonlinear relation between the battery capacity (A.H.) and the average current was also defined. For multi-cell systems, it was shown that using the parallel configuration is better than serial or alternating configurations. We also introduced a modification to Rakhmatov's diffusion model. Our modification allows the simulation of any discharge current profile and not only pulsed discharge profiles. We had also introduced a new hybrid battery model that combines both the electric circuit characteristics of the comprehensive electric circuit model and the nonlinear battery properties of Rakhmatov Diffusion Model.

VII. PUBLICATIONS

1. “New Hybrid Battery Model that take into both electric circuit characteristics and non linear properties”. In preparation.
2. “Battery lifetime optimization techniques”. In preparation

VIII. REFERENCES

[1] Jongerden, M.R.; Haverkort, B.R., "Which battery model to use?" *Software, IET* ,vol.3,no.6,pp.445,457,December 2009.
URL: http://ieeexplore.ieee.org/stamp/stamp.jsp?tp=&arnumber=5346550&isnumber=5346548

[2] Lahiri, K.; Raghunathan, A.; Dey, S.; Panigrahi, D., "Battery-driven system design: a new frontier in low power design," *Design Automation Conference, 2002. Proceedings of ASP-DAC 2002. 7th Asia and South Pacific and the 15th International Conference on VLSI Design. Proceedings.* , vol., no., pp.261,267, 2002.
URL: http://ieeexplore.ieee.org/stamp/stamp.jsp?tp=&arnumber=994932&isnumber=21450

[3] Rakhmatov, D.; Vrudhula, S.; Wallach, D.A., "A model for battery lifetime analysis for organizing applications on a pocket computer," *IEEE Transactions on Very Large Scale Integration (VLSI) Systems"*, vol.11, no.6, pp.1019,1030, Dec. 2003.
URL: http://ieeexplore.ieee.org/stamp/stamp.jsp?tp=&arnumber=1255477&isnumber=28080

[4] Peng Rong; Pedram, M., "Battery-aware power management based on Markovian decision processes," *IEEE Transactions on Computer-Aided Design of Integrated Circuits and Systems"*, vol.25,no.7,pp.1337,1349,July2006.
URL: http://ieeexplore.ieee.org/stamp/stamp.jsp?tp=&arnumber=1634629&isnumber=34277

[5] Min Chen; Rincon-Mora, G.A., "Accurate electrical battery model capable of predicting runtime and I-V performance," *IEEE Transactions on Energy Conversion"* , vol.21, no.2, pp.504,511,June2006.
URL: http://ieeexplore.ieee.org/stamp/stamp.jsp?tp=&arnumber=1634598&isnumber=34276

[6] Dai Haifeng; Wei Xuezhe; Sun Zechang, "A new SOH prediction concept for the power lithium-ion battery used on HEVs," *Vehicle Power and Propulsion Conference, 2009. VPPC '09. IEEE* , vol., no., pp.1649,1653, 7-10 Sept. 2009.
URL: http://ieeexplore.ieee.org/stamp/stamp.jsp?tp=&arnumber=5289654&isnumber=5289440

[7] Coleman, M.; Lee, C.K.; Hurley, W.G., "State of Health Determination: Two Pulse Load Test for a VRLA Battery," *Power Electronics Specialists Conference, 2006. PESC '06. 37th IEEE* , vol., no., pp.1,6, 18-22 June 2006.
URL: http://ieeexplore.ieee.org/stamp/stamp.jsp?tp=&arnumber=1711801&isnumber=36090

[8] Rao, R.; Vrudhula, S.; Rakhmatov, D.N., "Battery modeling for energy aware system design," *Computer* , vol.36, no.12, pp.77,87, Dec. 2003.
URL: http://ieeexplore.ieee.org/stamp/stamp.jsp?tp=&arnumber=1250886&isnumber=27996

[9] H. Kim, "Dynamic Battery modeling in hybrid electric vehicles," Master thesis, The Ohio State University, 2002.

[10] Lijun Gao; Liu, Shengyi; Dougal, R.A., "Dynamic lithium-ion battery model for system simulation," *IEEE Transactions on Components and Packaging Technologies"*, vol.25, no.3, pp.495,505, Sep 2002.
URL: http://ieeexplore.ieee.org/stamp/stamp.jsp?tp=&arnumber=1159187&isnumber=25974

[11] M. Doyle, T. F. Fuller, and J. Newman, "Modeling of galvanostatic charge and discharge of the lithium/polymer/insertion cell," *J. Electrochem. Soc*., vol. 140, no. 6, pp. 1526–1533, Jun. 1993.

[12] Salameh, Z.M.; Casacca, M.A.; Lynch, William A., "A mathematical model for lead-acid batteries," *Energy Conversion, IEEE Transactions on* , vol.7, no.1, pp.93,98, Mar 1992.

URL: http://ieeexplore.ieee.org/stamp/stamp.jsp?tp=&arnumber=124547&isnumber=3515

[13] Valvo, M.; Wicks, F.E.; Robertson, D.; Rudin, S., "Development and application of an improved equivalent circuit model of a lead acid battery," *Energy Conversion Engineering Conference, 1996. IECEC 96., Proceedings of the 31st Intersociety* , vol.2, no., pp.1159,1163 vol.2, 11-16 Aug 1996.
URL: http://ieeexplore.ieee.org/stamp/stamp.jsp?tp=&arnumber=553872&isnumber=11980

[14] Ceraolo, M., "New dynamical models of lead-acid batteries," *Power Systems, IEEE Transactions on* , vol.15, no.4, pp.1184,1190, Nov 2000.
URL: http://ieeexplore.ieee.org/stamp/stamp.jsp?tp=&arnumber=898088&isnumber=19443

[15] Barsali, Stefano; Ceraolo, M., "Dynamical models of lead-acid batteries: implementation issues," *Energy Conversion, IEEE Transactions on* , vol.17, no.1, pp.16,23, Mar 2002.
URL: http://ieeexplore.ieee.org/stamp/stamp.jsp?tp=&arnumber=986432&isnumber=21257

[16] Lijun Gao; Liu, Shengyi; Dougal, R.A., "Dynamic lithium-ion battery model for system simulation," *Components and Packaging Technologies, IEEE Transactions on* , vol.25, no.3, pp.495,505, Sep 2002.
URL: http://ieeexplore.ieee.org/stamp/stamp.jsp?tp=&arnumber=1159187&isnumber=25974

[17] Glass, M.C., "Battery electrochemical nonlinear/dynamic SPICE model," *Energy Conversion Engineering Conference, 1996. IECEC 96., Proceedings of the 31st Intersociety* , vol.1, no., pp.292,297 vol.1, 11-16 Aug 1996.
URL: http://ieeexplore.ieee.org/stamp/stamp.jsp?tp=&arnumber=552887&isnumber=11973

[18] Buller, S.; Thele, M.; De Doncker, R.W.; Karden, E., "Impedance-based simulation models of supercapacitors and Li-ion batteries for power electronic applications," *Industry Applications Conference, 2003. 38th IAS Annual Meeting. Conference Record of the* , vol.3, no., pp.1596,1600 vol.3, 12-16 Oct. 2003.
URL: http://ieeexplore.ieee.org/stamp/stamp.jsp?tp=&arnumber=1257769&isnumber=28118

[19] Chiasserini, C.F. ; Rao, R., "Pulsed battery discharge in communication devices," Proceedings of the 5th annual ACM/IEEE international conference on Mobile computing and networking, p.88-95, August 15-19, 1999.

[20] Tsang, K.M.; Chan, W.L.; Wong, Y.K.; Sun, L., "Lithium-ion battery models for computer simulation," *Automation and Logistics (ICAL), 2010 IEEE International Conference on* , vol., no., pp.98,102, 16-20 Aug. 2010.
URL: http://ieeexplore.ieee.org/stamp/stamp.jsp?tp=&arnumber=5585392&isnumber=5585273

[21] Rao, V.; Singhal, G.; Kumar, A.; Navet, N., "Battery model for embedded systems," *VLSI Design, 2005. 18th International Conference on* , vol., no., pp.105,110, 3-7 Jan. 2005.
URL: http://ieeexplore.ieee.org/stamp/stamp.jsp?tp=&arnumber=1383261&isnumber=30140

[22] Chiasserini, C.; Rao, R.R., "Energy efficient battery management," *Selected Areas in Communications, IEEE Journal on* , vol.19, no.7, pp.1235,1245, Jul 2001.
URL: http://ieeexplore.ieee.org/stamp/stamp.jsp?tp=&arnumber=932692&isnumber=20181

[23] MANWELL J., MCGOWAN J., "Lead acid battery storage model for hybrid energy systems," Solar Energy, pp. 399–405, 1993.

[24] MANWELL J., MCGOWAN J., "Extension of the kinetic battery model for wind/hybrid power systems," Proc. Fifth European Wind Energy Association Conf. (EWEC '94), pp. 284–289, 1994.

[25] MANWELL J., MCGOWAN J., BARING-GOULD E., S.W., LEOTTA A., “Evaluation of battery models for wind/hybrid power system simulation,”. Proc. fifth European Wind Energy Association Conference (EWEC ’94), pp. 1182–1187, 1994.

[26] Jiong Luo; Jha, N.K., "Battery-aware static scheduling for distributed real-time embedded systems," *Design Automation Conference, 2001. Proceedings* , vol.,no.,pp.444,449,2001.
URL: http://ieeexplore.ieee.org/stamp/stamp.jsp?tp=&arnumber=935550&isnumber=20239

[27] Rakhmatov, D.; Vrudhula, S.; Chakrabarti, C., "Battery-conscious task sequencing for portable devices including voltage/clock scaling," *Design Automation Conference, 2002. Proceedings. 39th* , vol., no., pp.189,194, 2002.
URL: http://ieeexplore.ieee.org/stamp/stamp.jsp?tp=&arnumber=1012618&isnumber=21813

[28] Benini, L.; Castelli, G.; Macii, A.; Macii, E.; Poncino, M.; Scarsi, R., "Extending lifetime of portable systems by battery scheduling," *Design, Automation and Test in Europe, 2001. Conference and Exhibition 2001. Proceedings* , vol., no., pp.197,201, 2001.
URL: http://ieeexplore.ieee.org/stamp/stamp.jsp?tp=&arnumber=915024&isnumber=19761

[29] Mandal, S.K.; Bhojwani, P.S.; Mohanty, S.P.; Mahapatra, R.N., "IntellBatt: Towards smarter battery design," *Design Automation Conference, 2008. DAC 2008. 45th ACM/IEEE* , vol., no., pp.872,877, 8-13 June 2008.
URL: http://ieeexplore.ieee.org/stamp/stamp.jsp?tp=&arnumber=4555942&isnumber=4555759

APPENDIX A

Expression Used in Cadence to Evaluate Equation 18:

Equation 18: $SOC = 100 - 100 * \frac{(\int_0^L i(\tau)d\tau + 2\sum_{m=1}^{10} e^{CF-\beta^2 m^2 L} \int_0^L i(\tau) e^{\beta^2 m^2 \tau - CF} d\tau)}{\alpha}$

Cadence Expression:

100 - 100 * (iinteg(IT("/V0/MINUS")) + 2*(

exp(VAR("CF")*0.01 - 0.001296 * xval(IT("/V0/MINUS")))*iinteg(IT("/V0/MINUS")*exp(0.001296 * xval(IT("/V0/MINUS")) - VAR("CF")*0.01))

+exp(VAR("CF")*0.04 - 0.001296 *4* xval(IT("/V0/MINUS")))*iinteg(IT("/V0/MINUS")*exp(0.001296 *4* xval(IT("/V0/MINUS")) - VAR("CF")*0.04))

+exp(VAR("CF")*0.09 - 0.001296 *9* xval(IT("/V0/MINUS")))*iinteg(IT("/V0/MINUS")*exp(0.001296 *9* xval(IT("/V0/MINUS")) - VAR("CF")*0.09))

+exp(VAR("CF")*0.16 - 0.001296 *16* xval(IT("/V0/MINUS")))*iinteg(IT("/V0/MINUS")*exp(0.001296 *16* xval(IT("/V0/MINUS")) - VAR("CF")*0.16))

+exp(VAR("CF")*0.25 - 0.001296 *25* xval(IT("/V0/MINUS")))*iinteg(IT("/V0/MINUS")*exp(0.001296 *25* xval(IT("/V0/MINUS")) - VAR("CF")*0.25))

+exp(VAR("CF")*0.36 - 0.001296 *36* xval(IT("/V0/MINUS")))*iinteg(IT("/V0/MINUS")*exp(0.001296 *36* xval(IT("/V0/MINUS")) - VAR("CF")*0.36))

+exp(VAR("CF")*0.49 - 0.001296 *49* xval(IT("/V0/MINUS")))*iinteg(IT("/V0/MINUS")*exp(0.001296 *49* xval(IT("/V0/MINUS")) - VAR("CF")*0.49))

+exp(VAR("CF")*0.64 - 0.001296 *64* xval(IT("/V0/MINUS")))*iinteg(IT("/V0/MINUS")*exp(0.001296 *64* xval(IT("/V0/MINUS")) - VAR("CF")*0.64))

+exp(VAR("CF")*0.81 - 0.001296 *81* xval(IT("/V0/MINUS")))*iinteg(IT("/V0/MINUS")*exp(0.001296 *81* xval(IT("/V0/MINUS")) - VAR("CF")*0.81))

+exp(VAR("CF")*1.00 - 0.001296 *100* xval(IT("/V0/MINUS")))*iinteg(IT("/V0/MINUS")*exp(0.001296 *100* xval(IT("/V0/MINUS"))- VAR("CF")*1.00))

))/2418.5

LMS Algorithm for determining α & β

T11 through T22 are constant work loads that were simulated in [3]. We used those data in order to get α and β. The below table shows the measured life times and their corresponding average currents. Then we calculated the term β^2 L in equation 12.

	T11	T12	T13	T14	T15	T16	T17	T18	T19	T20	T21	T22
L (min)	26.6	41.4	53.9	96.7	110.6	118.6	131.0	251.3	313.0	659.5	1201.0	93.2
L (sec)	1596	2484	3234	5802	6636	7116	7860	15078	18780	39570	72060	5592
I(A)	0.6	0.5	0.4	0.3	0.3	0.3	0.2	0.1	0.1	0.1	0.0	0.3
β^2 L	2.1	3.2	4.2	7.5	8.6	9.2	10.2	19.5	24.3	51.3	93.4	7.2

$$\alpha = IL\left[1 + 2\sum_{m=1}^{\infty}\frac{1-e^{-\beta^2 m^2 L}}{\beta^2 m^2 L}\right] \quad \text{Equation 34}$$

In the table below, we are calculating the first 20 terms of the summation then at the end of the table we are obtaining the α for each profile.

Summation Term #	T11	T12	T13	T14	T15	T16	T17	T18	T19	T20	T21	T22
1	0.42236	0.29821	0.23498	0.13292	0.11625	0.10842	0.09816	0.05117	0.04109	0.0195	0.01071	0.13789
2	0.12083	0.07766	0.05965	0.03325	0.02907	0.02711	0.02454	0.01279	0.01027	0.00487	0.00268	0.0345
3	0.05372	0.03451	0.02651	0.01478	0.01292	0.01205	0.01091	0.00569	0.00457	0.00217	0.00119	0.01533
4	0.03022	0.01941	0.01491	0.00831	0.00727	0.00678	0.00614	0.0032	0.00257	0.00122	0.00067	0.00862
5	0.01934	0.01243	0.00954	0.00532	0.00465	0.00434	0.00393	0.00205	0.00164	0.00078	0.00043	0.00552
6	0.01343	0.00863	0.00663	0.00369	0.00323	0.00301	0.00273	0.00142	0.00114	0.00054	0.0003	0.00383
7	0.00987	0.00634	0.00487	0.00271	0.00237	0.00221	0.002	0.00104	0.00084	0.0004	0.00022	0.00282
8	0.00755	0.00485	0.00373	0.00208	0.00182	0.00169	0.00153	0.0008	0.00064	0.0003	0.00017	0.00216
9	0.00597	0.00383	0.00295	0.00164	0.00144	0.00134	0.00121	0.00063	0.00051	0.00024	0.00013	0.0017
10	0.00483	0.00311	0.00239	0.00133	0.00116	0.00108	0.00098	0.00051	0.00041	0.00019	0.00011	0.00138
11	0.004	0.00257	0.00197	0.0011	0.00096	0.0009	0.00081	0.00042	0.00034	0.00016	0.00009	0.00114
12	0.00336	0.00216	0.00166	0.00092	0.00081	0.00075	0.00068	0.00036	0.00029	0.00014	0.00007	0.00096
13	0.00286	0.00184	0.00141	0.00079	0.00069	0.00064	0.00058	0.0003	0.00024	0.00012	0.00006	0.00082
14	0.00247	0.00158	0.00122	0.00068	0.00059	0.00055	0.0005	0.00026	0.00021	0.0001	0.00005	0.0007
15	0.00215	0.00138	0.00106	0.00059	0.00052	0.00048	0.00044	0.00023	0.00018	0.00009	0.00005	0.00061
16	0.00189	0.00121	0.00093	0.00052	0.00045	0.00042	0.00038	0.0002	0.00016	0.00008	0.00004	0.00054
17	0.00167	0.00107	0.00083	0.00046	0.0004	0.00038	0.00034	0.00018	0.00014	0.00007	0.00004	0.00048
18	0.00149	0.00096	0.00074	0.00041	0.00036	0.00033	0.0003	0.00016	0.00013	0.00006	0.00003	0.00043
19	0.00134	0.00086	0.00066	0.00037	0.00032	0.0003	0.00027	0.00014	0.00011	0.00005	0.00003	0.00038
20	0.00121	0.00078	0.0006	0.00033	0.00029	0.00027	0.00025	0.00013	0.0001	0.00005	0.00003	0.00034
∑	2.4211	1.96679	1.75444	1.4244	1.37115	1.34613	1.31338	1.16336	1.13116	1.06225	1.03418	1.44029
α	2426.64	2416.86	2414.8	2415.68	2416.68	2416.8	2416.65	2418.93	2419.6	2421.11	2422	2416.23

We varied the value of the β used in the equation till we could get the least possible standard deviation σ for α among the all workloads.

	μ	σ
α	2418.4993	3.383053
β	0.036	

APPENDIX B

Below are the schematics that were used to implement the hybrid battery model in Cadence.

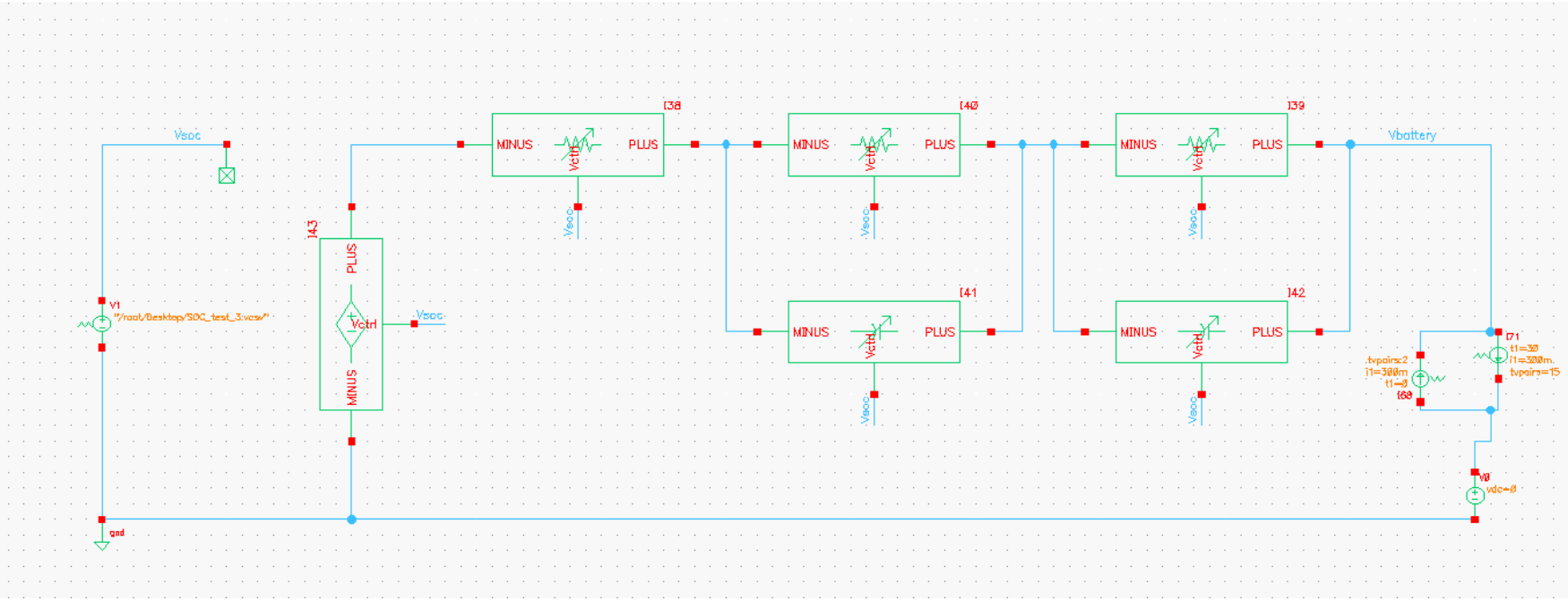

Figure 26: Hybrid Battery Model

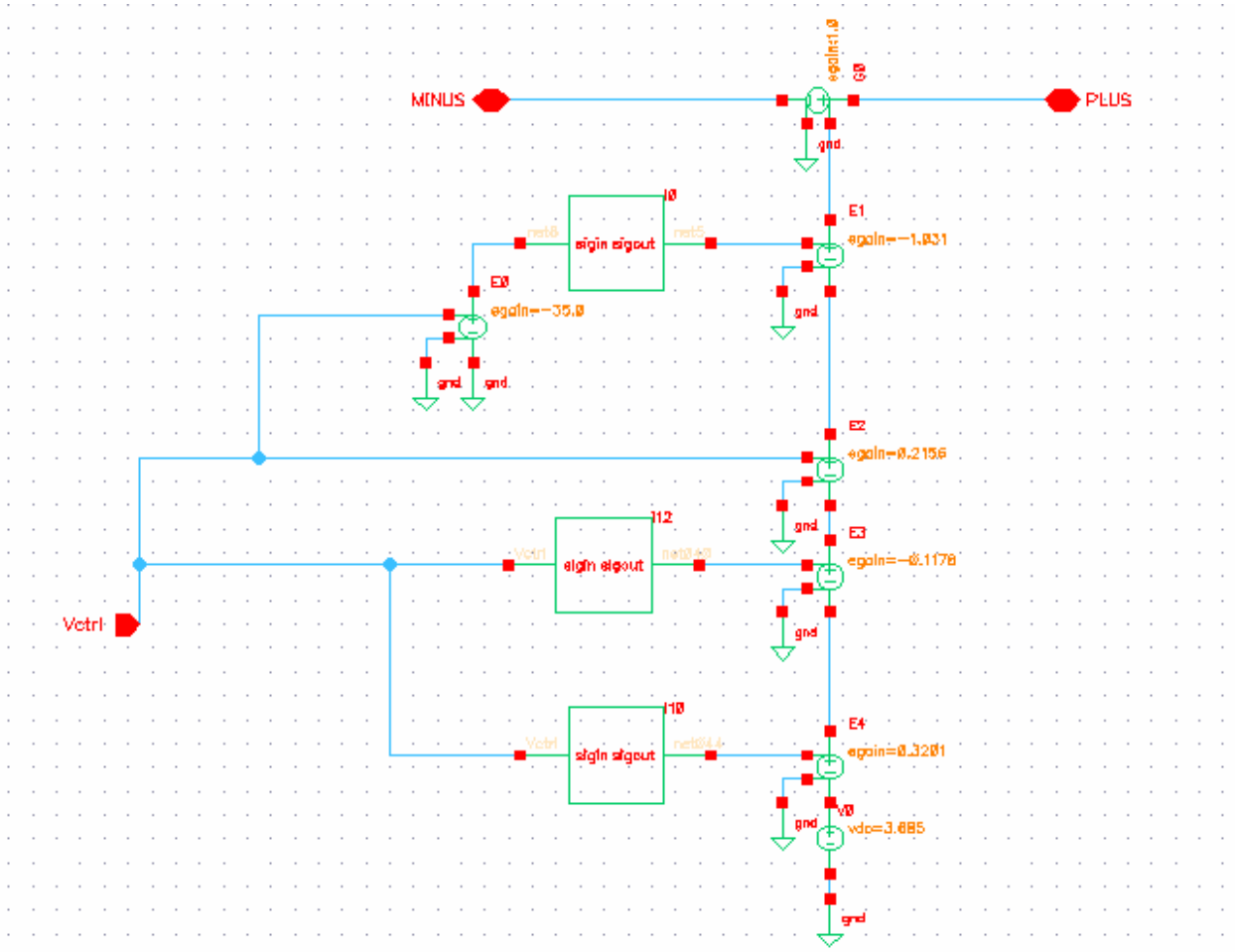

Figure 27: V_{oc}(SOC) of the Hybrid Model

$$\mathbf{V_{OC}(SOC) = -a_1 . e^{-a_2 . SOC} + a_3 + a_4 . SOC - a_5 . SOC^2 + a_6 . SOC^3}$$

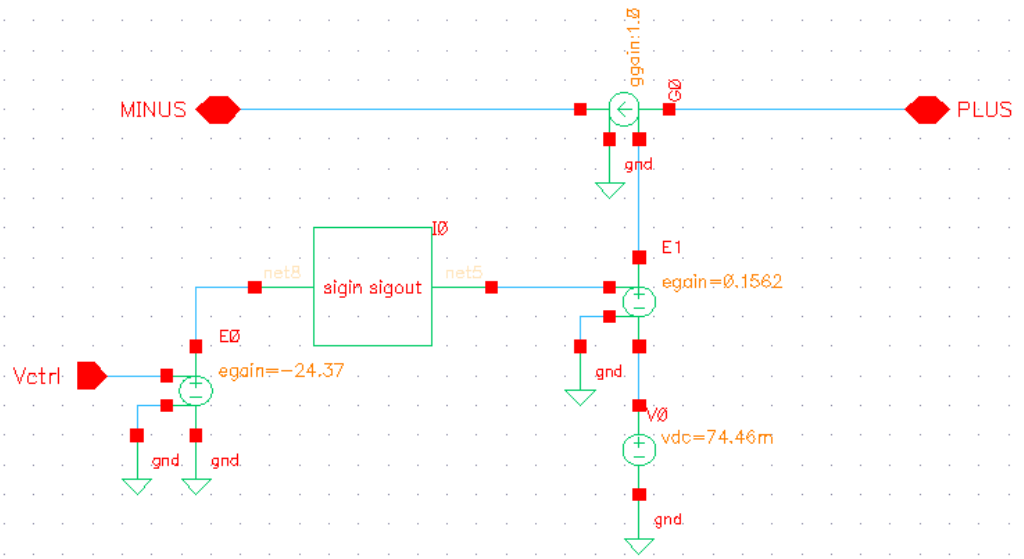

Figure 28: R_{series} of the Hybrid Model

$$\mathbf{R_{series}(SOC) = b_1 . e^{-b_2 . SOC} + b_3}$$

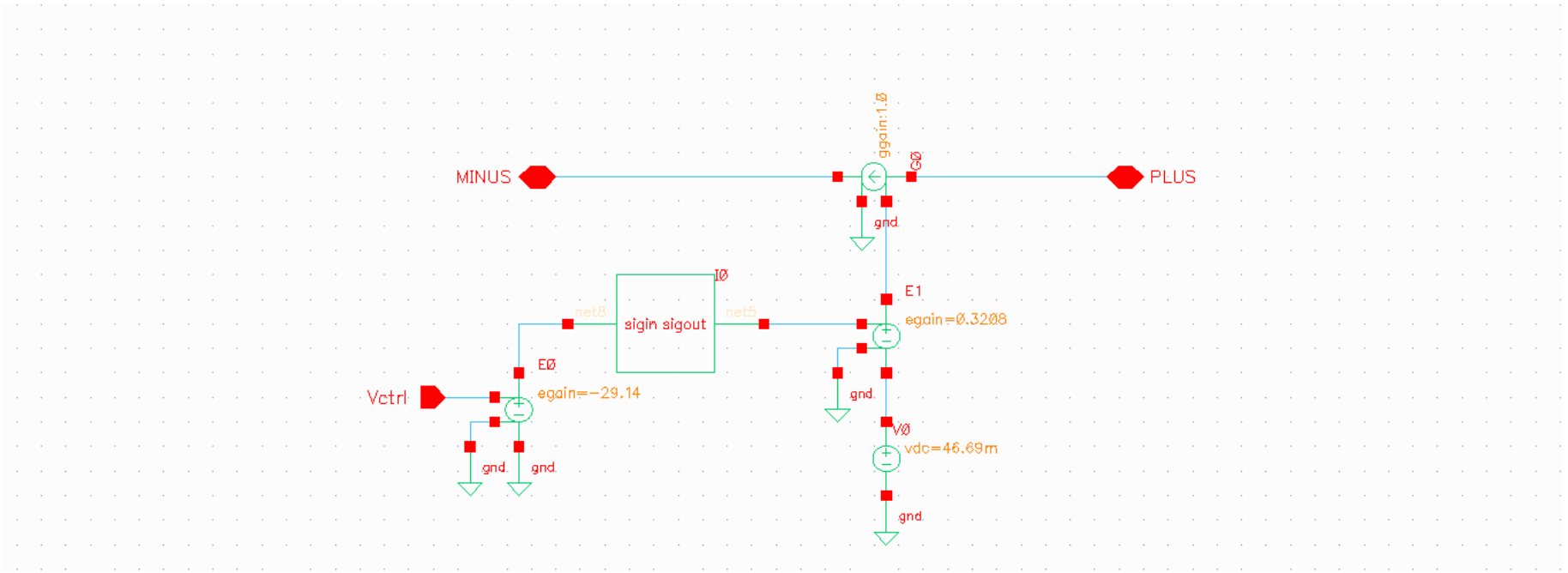

Figure 29: $R_{transient\_S}$ of the Hybrid Battery Model

$$\mathbf{R_{Transient\_S}(SOC) = c_1 . e^{-c_2 . SOC} + c_3}$$

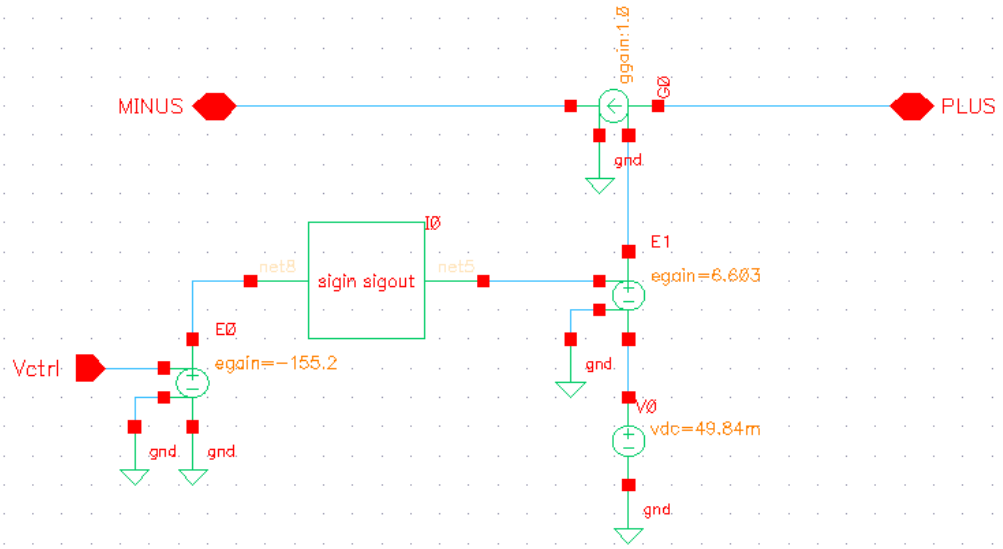

Figure 30: $R_{transient\_L}$ of the Hybrid Battery Model

$$\mathbf{R_{Transient\_L}(SOC) = f_1 . e^{-f_2 . SOC} + f_3}$$

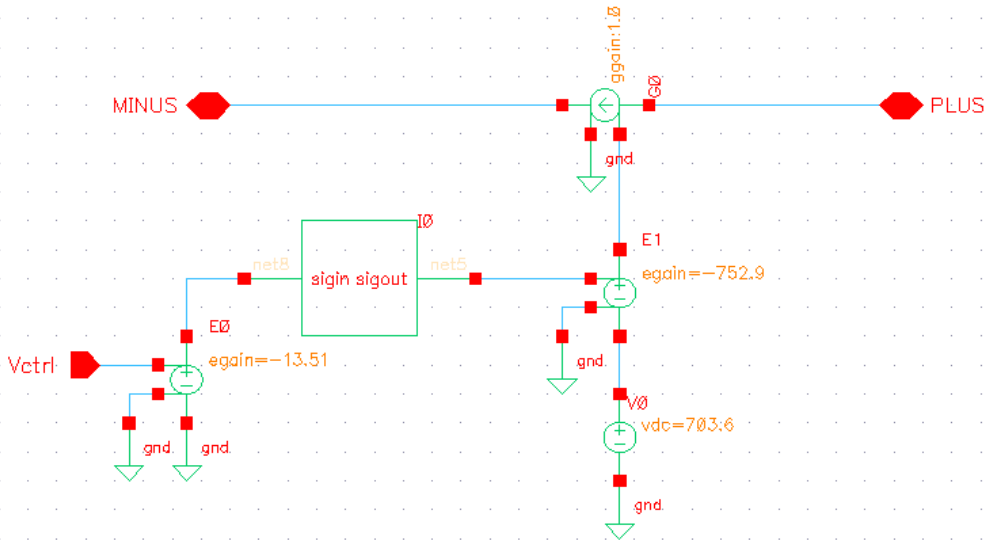

Figure 31:$C_{transient\_s}$ of the Hybrid Battery Model

$$\mathbf{C_{Transient\_S}(SOC) = -d_1 . e^{-d_2 . SOC} + d_3}$$

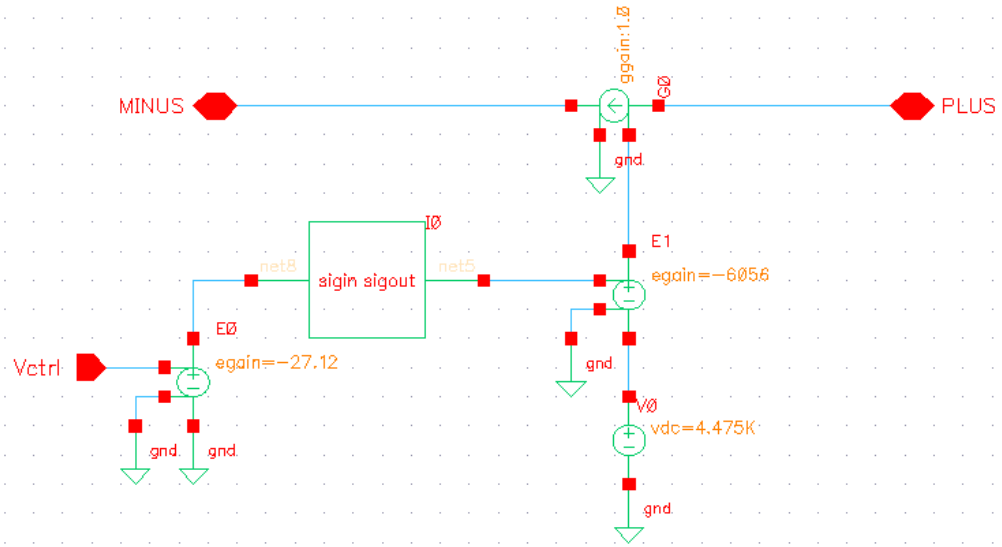

Figure 32: Ctransient_L of the Hybrid Battery Model

$$\mathbf{C_{Transient\_L}(SOC) = -g_1 . e^{-g_2 . SOC} + g_3}$$